Received: 5 June 2024 | Accepted: 5 July 2025

DOI: 10.1111/jpy.70069

RESEARCH ARTICLE

Biochemical characterization of phosphoenolpyruvate carboxykinases from multiple species of brown algae

Jian-qiang Jin[1] | **Yuusuke Yokooji**[1] | **Toshiyuki Shibata**[2] | **Haruyuki Atomi**[1,3]

[1]Department of Synthetic Chemistry and Biological Chemistry, Graduate School of Engineering, Kyoto University, Kyoto, Japan

[2]Center for Global Environment Education & Research, Mie University, Tsu, Mie, Japan

[3]Integrated Research Center for Carbon Negative Science, Kyoto University, Uji, Japan

Correspondence
Haruyuki Atomi, Department of Synthetic Chemistry and Biological Chemistry, Graduate School of Engineering, Kyoto University, Katsura, Nishikyo-ku, Kyoto, Japan.
Email: atomi.haruyuki.8r@kyoto-u.ac.jp

Funding information
New Energy and Industrial Technology Development Organization, Grant/Award Number: JPNP18016

Editor: D. Petroutsos

Abstract

Phosphoenolpyruvate carboxykinase (PEPCK) is involved in the conversion of phosphoenolpyruvate (PEP) to oxaloacetate (OAA). In addition to playing a role in gluconeogenesis in various organisms, PEPCK also functions in the C_4 cycle to concentrate CO_2 for photosynthesis in some C_4 plants. Brown algae harbor genes related to the C_4 cycle, including the PEPCK gene, and are proposed to employ a C_4 cycle-like pathway. However, little is known about the CO_2-concentrating mechanisms and the properties of the enzymes involved in brown algae. Here, we obtained soluble recombinant PEPCKs of five brown algae and carried out biochemical analyses. The five PEPCKs were ATP-dependent and displayed similar or higher specific activities compared with their counterparts from other organisms. Phosphoenolpyruvate carboxykinase from *Ishige okamurae* (*Io*-PEPCK) exhibited the highest specific activity in both carboxylation and decarboxylation directions, with values of 48.4 and 63.3 μmol · min^{-1} · mg^{-1}, respectively. Additionally, *Io*-PEPCK displayed a k_{cat}/K_{mHCO3} value of 9.2×10^3 · M^{-1} · s^{-1}, much higher than those of previously characterized PEPCKs. The response of PEPCK activity to various metabolites showed that citrate and malate inhibited the carboxylation but promoted the decarboxylation activity of *Io*-PEPCK. Various ATP concentrations resulted in different degrees of inhibition on the carboxylation activity of PEPCK, suggesting that ATP concentration potentially regulates PEPCK activity in brown algae. The analysis of cell extracts from *I. okamurae* suggested that PEPCK rather than PEPC dominates the carboxylation in this brown alga. Based on previous knowledge and the results presented here, a model for a C_4 cycle-like pathway in brown algae has been proposed.

KEYWORDS
brown algae, carbon dioxide, carbon dioxide enrichment, carbon fixation, kelp, macroalgae, phosphoenolpyruvate carboxykinase

INTRODUCTION

The carbon sequestered by coastal vegetated ecosystems is known as "blue carbon" and is increasingly being positioned as a practical climate change mitigation measure (Duarte et al., 2013; Nellemann et al., 2009). Macroalgae in these ecosystems have particularly high carbon sequestration capacities, so marine coastal ecosystems with macroalgae as primary producers, which are called "macroalgal forests," have recently

Abbreviations: 3-PGA, 3-phosphoglycerate; CAM, crassulacean acid metabolism; CBB, Calvin–Benson–Bassham; CCM, CO_2-concentrating mechanism; DTT, dithiothreitol; FBP, fructose 1,6-bisphosphate; G6P, glucose 6-phosphate; HPLC, high-performance liquid chromatography; K_{av}, partition coefficient; k_{cat}, turnover number; LDH, lactate dehydrogenase; MDH, malate dehydrogenase; OAA, oxaloacetate; PCR, polymerase chain reaction; PEP, phosphoenolpyruvate; PEPC, phosphoenolpyruvate carboxylase; PEPCK, phosphoenolpyruvate carboxykinase; PK, pyruvate kinase; PMSF, phenylmethylsulfonyl fluoride; PPi, pyrophosphate; RuBisCO, ribulose-1,5-bisphosphate carboxylase/oxygenase.

been identified as one of the largest contributors to carbon sequestration on Earth (Duarte et al., 2013; Duarte et al., 2022; Griscom et al., 2017; Krause-Jensen & Duarte, 2016; Pessarrodona et al., 2023). It has been estimated that 61 to 268 Tg (10^{12} g) of carbon per year is sequestered in deep sea and coastal soil (Krause-Jensen & Duarte, 2016). Efforts have been made to model the pathways of carbon sequestered by macroalgal ecosystems and to develop methods to accurately assess their fluxes in order to incorporate this blue carbon into an international carbon trading framework.

Carbon dioxide fixation in organisms, including plants, algae, and cyanobacteria, is carried out through the function of ribulose-1,5-bisphosphate carboxylase/oxygenase (RuBisCO) and the Calvin–Benson–Bassham (CBB) cycle. In many organisms, CO_2-concentrating mechanisms (CCMs) are also present, providing a high concentration of CO_2 to RuBisCO (Koch et al., 2013; Maberly & Gontero, 2017; Meyer & Griffiths, 2013; Raven & Giordano, 2017). The CCMs are broadly classified into biophysical CCMs and biochemical CCMs (Maberly & Gontero, 2017; Raven & Giordano, 2017). Biophysical CCMs consist of active transport and interconversion of CO_2 and HCO_3^- by transporters and carbonic anhydrase activities and condensation of enzymes such as RuBisCO by the formation of carboxysomes and pyrenoids. Biochemical CCMs contain metabolic pathways, such as those found in C_4 photosynthesis and crassulacean acid metabolism (CAM). In C_4 plants, initial fixation of atmospheric CO_2 occurs in mesophyll cells by phosphoenolpyruvate carboxylase (PEPC), converting CO_2 and phosphoenolpyruvate (PEP) to oxaloacetate (OAA) in an irreversible manner. Oxaloacetate is then converted to malate (Figure S1a) or aspartate (Figure S1b,c) and transported to bundle-sheath cells, in which they are converted so that CO_2 is released and can be provided to RuBisCO. C_4 cycles are classified into three subtypes based on the different decarboxylation modes or enzymes used to release CO_2: NADP-malic enzyme type (Figure S1a), NAD-malic enzyme type (Figure S1b), and PEP carboxykinase (PEPCK) type (Figure S1c; Furbank, 2011, 2016; Rao & Dixon, 2016; Wang et al., 2014). The NADP-malic enzyme type metabolism stores the C_4 compounds as malate, whereas the other two types store the C_4 compounds as aspartate (Figure S1). Regardless of the enzyme that carries out decarboxylation, PEPC is the enzyme responsible for the initial carboxylation in the CCM of C_4 plants.

Carbon concentration mechanisms are also presumed to function in macroalgae, particularly in brown algae (Phaeophyceae; Koch et al., 2013; Maberly & Gontero, 2017; Meyer & Griffiths, 2013; Raven & Giordano, 2017). The apparent function of CCMs has been observed in a wide range of brown algae, but this is not necessarily the case in red algae (Stepien et al., 2016). Although CCMs require energy, active CO_2 uptake by the underwater algae is important for their RuBisCOs to reach full potential. The average dissolved CO_2 concentration in seawater (15 μM) is thought to be insufficient to inhibit the oxygenase activity of RuBisCO in brown algae, and the gas diffusion rate of CO_2 in water is very slow (1/10,000 of that in the atmosphere, $2\times10^{-9}\,m^2\cdot s^{-1}$ 1 atm 25°C; Koch et al., 2013; Maberly & Gontero, 2017; Oh et al., 2023). Indeed, an inverse correlation has been observed between the efficiency of CCMs and the CO_2 fixation efficiency of RuBisCO among algae, suggesting that CCMs influence the kinetic evolution of their RuBisCOs (Capó-Bauçà et al., 2023; Capó-Bauçà et al., 2024; Iñiguez et al., 2020; Maberly & Gontero, 2017).

Although PEPCK is involved in the release of CO_2 in plants that utilize the PEPCK-type C_4 cycle (Figure S1c,d), the PEPCK reaction is reversible (Figure 1), and thus in principle, PEPCK can also function as a carbon-fixing enzyme. Carboxylation activity of PEPCK has been detected in the extracts of multiple species of brown algae (Akagawa et al., 1972a; Busch & Schmid, 2001; Cabello-Pasini et al., 2000; Cabello-Pasini & Alberte, 2001b; Gravot et al., 2010; Johnston & Raven, 1989; Kremer, 1981b; Kremer & Kuppers, 1977). In the 1960s–1980s, high carbon-fixation activities by PEPCK under dark conditions were detected in macroalgae and considered to be involved in "light-independent CO_2-fixation" or "dark fixation," independent of RuBisCO and the CBB cycle (Akagawa et al., 1972a, 1972b; Akagawa, Nisizawa, & Ikawa, 1972; Cabello-Pasini & Alberte, 1997; Craigie, 1963; Holbrook et al., 1988; Johnston & Raven, 1989; Joshi et al., 1962;

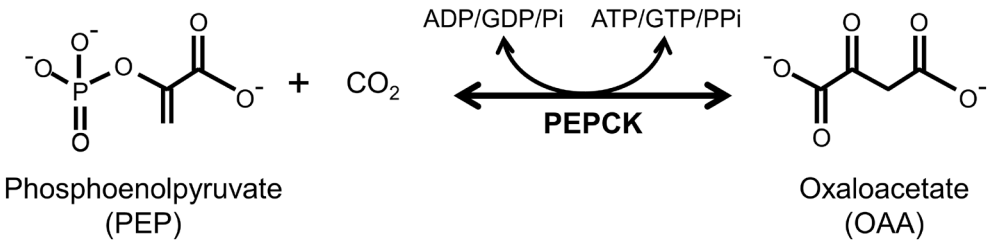

FIGURE 1 The reaction catalyzed by PEPCK. PEPCK catalyzes the ADP/GDP/Pi-dependent carboxylation of phosphoenolpyruvate (PEP) and ATP/GTP/PPi-dependent decarboxylation of oxaloacetate (OAA).

Kremer, 1981a, 1981b; Kremer & Kuppers, 1977; Willenbrink et al., 1975). PEPCK carboxylating activities were at comparable levels in both light and dark conditions (Akagawa, Nisizawa, & Ikawa, 1972; Kremer, 1981a, 1981b; Kremer & Kuppers, 1977), which was distinct to the behavior of PEPC carboxylation and PEPCK decarboxylation in the C_4 pathway. It has also been reported that the ratio of PEPCK carboxylase activity to RuBisCO activity varied with the distance of the blades from the meristem (growing zone of the thallus), with PEPCK carboxylating activity being highest at the meristem (Cabello-Pasini & Alberte, 2001a, 2001b; Gómez et al., 2007; Kremer, 1981b; Willenbrink et al., 1975). PEPCK contributed up to 10% of the total carboxylation capacity of brown algae but accounted for nearly half of the carboxylation capacity in the growing zone of the thallus (Gómez & Huovinen, 2012; Kremer, 1981b; Kremer & Kuppers, 1977). It was reported that the CO_2-fixation rate of PEPCK under dark conditions accounted for merely 50% of the carbon loss rate due to dark respiration (O_2 consumption), much lower than the case of PEPC in CAM plants (Gómez & Huovinen, 2012; Kremer, 1981b). Therefore, light-independent CO_2-fixation by PEPCK in brown algae is not expected to have as high a flux as those observed in the PEPC-dependent C_4 and CAM pathways (Koch et al., 2013; Raven & Giordano, 2017).

Concerning PEPC, a gene annotated as PEPC is present in the genome of *Ectocarpus siliculosus* (Cock et al., 2010; Gravot et al., 2010), and quantitative reverse transcription polymerase chain reaction (qRT-PCR) analysis has confirmed the presence of PEPC transcripts in *Saccharina japonica* (Shao et al., 2019), suggesting that these brown algae harbor PEPC. In the brown algae *Eisenia bicyclis*, *Dictyota dichotoma*, and *Spatoglossum pacificum*, fixed carbon is initially stored in the form of aspartate with no immediate generation of malate (Akagawa, Ikawa, & Nisizawa, 1972b), resembling the metabolism of the NAD-malic enzyme type (Figure S1b) and the PEPCK type (Figure S1c) C_4-pathways. However, interestingly, in previous studies on biochemical CCMs in brown algae, PEPC activity, which is usually the enzyme responsible for carboxylation in the C_4 pathway (Figure S1), was not detected in the extracts, except in that of *Dictyota guineensis* (Holbrook et al., 1988). Furthermore, predictions of the subcellular localization of PEPC and PEPCK based on primary structure have contradicted the classical C_4 and CAM pathways in plants (Chi et al., 2014; Shao et al., 2019). Although the observations described above raise the possibility that PEPCKs in brown algae play roles that differ from those proposed in classical C_4-pathways, such as the carboxylation of PEP rather than the decarboxylation of OAA, the actual physiological role of PEPCK and its contributions to CO_2-fixation remain unclear.

Three types of PEPCK are known, and these types utilize ATP, GTP, or pyrophosphate (PPi) as the energy source. From a kinetic standpoint, ATP/GTP-dependent PEPCKs prefer the decarboxylation reaction, while PPi-dependent PEPCK prefers the carboxylation reaction (McLeod & Holyoak, 2021; McLeod & Holyoak, 2023). PEPCK activity measurement in the ammonium sulfate precipitation fraction of extracts of the brown algae *Ectocarpus siliculosus* showed 10-fold higher activity of ATP-dependent carboxylation than that of decarboxylation (Busch & Schmid, 2001). Although these reports add support to the possibility that PEPCK in brown algae functions as a carbon-fixing enzyme, there are only examples of enzymatic analysis of proteins partially purified from the brown algae *Ascophyllum nodosum* and *Ec. siliculosus* (Busch & Schmid, 2001; Johnston & Raven, 1989). Recently, a PEPCK gene from *Saccharina japonica* was expressed in *Escherichia coli* but was obtained in the form of inclusion bodies (Lin et al., 2025). Although PEPCK activity could be detected after a refolding process, the carboxylation activity of the refolded protein was low compared to the activity of the partially purified enzyme from *A. nodosum*. To gain insight on the biochemical properties of PEPCK in brown algae, in this study, PEPCK genes from five brown algae, including *Ec. siliculosus*, *Sargassum horneri*, *Saccharina japonica*, *Scytosiphon lomentaria*, and *Ishige okamurae*, were successfully expressed in *Escherichia coli*. Recombinant proteins were obtained in soluble form and were purified without denaturation. The biochemical properties of these enzymes were examined and compared with PEPCKs from other organisms. We further carried out analysis on PEPCK from *I. okamurae* (*Io*-PEPCK), which exhibited the highest specific activity among the five brown algae PEPCKs. Combined with the examination of carbon-fixing activity in cell extracts of *I. okamurae*, a PEPCK-based C_4 cycle-like pathway in brown algae has been proposed.

MATERIALS AND METHODS

Chemicals, strains, algal material, media, and culture conditions

Unless mentioned otherwise, chemical reagents were purchased from Nacalai Tesque (Kyoto, Japan) or Fujifilm Wako Pure Chemicals (Osaka, Japan). *Escherichia coli* DH5α (Takara Bio, Kusatsu, Japan) was used for plasmid construction, and *E. coli* BL21-CodonPlus(DE3)-RIL (Agilent Technologies, Santa Clara, CA, United States) was used for gene expression. These were cultivated in Luria-Bertani medium (10 g · L^{-1} tryptone, 5 g · L^{-1} yeast extract, and 5 g · L^{-1} NaCl) containing ampicillin (100 mg · L^{-1}). Chloramphenicol (30 mg · L^{-1}) was also added in the LB medium to cultivate the

E. coli BL21-CodonPlus(DE3)-RIL cells. The brown alga *Ishige okamurae* was collected at a time between 2:00 a.m. and 4:00 p.m. at low tide on July 21, 2024 (a spring tide day) along the coast (33°68′ N, 130°29′ E) of Shikanoshima Island in Fukuoka prefecture, Japan. The collected algal thallus was washed and then stored at −80°C until use.

Construction of gene expression plasmids

PEPCKs from five macroalgae *Ectocarpus siliculosus*, *Sargassum horneri*, *Saccharina japonica*, *Scytosiphon lomentaria*, and *Ishige okamurae* were selected to be analyzed in this study. The coding regions of these five PEPCK genes were commercially synthesized and provided in the cloning vector Twist (plasmids Twist-PEPCK(sp)-*Es*, -*Sh*, -*Sj*, -*Sl*, and -*Io*; Twist Bioscience, San Francisco, CA, United States). Codons were optimized for expression in *Escherichia coli*, and sequences that encode N-terminal 6× His-tags and NdeI-EcoRI restriction sites were included (Figures S2 and S3a). Since several algal PEPCKs have been observed to be localized in the mitochondrion or chloroplast, as mentioned above, the potential targeting peptide sequences of these macroalgal PEPCKs were predicted by TargetP-2.0 and DeepLoc 2.0. The expression plasmids were constructed as follows (Figure S3a). The predicted targeting peptide sequences were removed by inverse PCR using Twist-PEPCK(sp) plasmids as the templates and the primers listed in Table S1. After treatment with DpnI to remove the templates, the amplified PCR products were phosphorylated and self-ligated and then introduced into *E. coli* DH5a competent cells by heat shock treatment at 42°C for 45 s. After confirming the absence of unintended mutations by DNA sequencing analysis, the resulting plasmids (Twist-PEPCK) were digested with the restriction enzymes NdeI and EcoRI. The target PEPCK genes with regions encoding the His-tag and sticky ends were inserted into the expression vector pET21a(+) at the corresponding sites, resulting in the formation of the expression plasmids (pET21a-PEPCK). The T7 promoter and terminator sequences were used as the primer set to select positive transformants and confirm the presence of PEPCK genes in the constructed expression plasmids (Figure S3b). DNA sequencing analysis was also carried out to confirm the absence of unintended mutations in the expression plasmids.

Gene expression and purification of PEPCK recombinant proteins

The expression plasmids were individually introduced into *Escherichia coli* BL21-CodonPlus(DE3)-RIL by heat shock treatment at 42°C for 45 s. Transformants were cultivated at 37°C until OD_{660} reached 0.4–0.6, and gene expression was induced by the addition of IPTG at a final concentration of 0.05 mM. Cells were further cultivated at 16°C for 20 h, and collected (4°C, 5500 × *g*, 15 min). Cells were resuspended in 20 mM sodium phosphate buffer (pH 7.4) containing 500 mM NaCl, 20 mM imidazole, and 1 mM phenylmethylsulfonyl fluoride (PMSF) to prevent proteolysis. Mixtures were kept on ice, and cells were disrupted by sonication. After centrifugation (4°C, 13,000 × *g*, 15 min), the supernatant was loaded onto a His GraviTrap column (Cytiva, Marlborough, MA, United States). Proteins were eluted with elution buffer containing 20 mM sodium phosphate (pH 7.4), 500 mM NaCl, and 500 mM imidazole. After exchanging the buffer of the relevant fractions to 50 mM Tris–HCl (pH 7.5) using Amicon Ultra centrifugal filter unit (MWCO 10 K; EMD Millipore, Billerica, MA, United States), samples were individually applied to an anion-exchange column, Resource Q (GE Healthcare, Little Chalfont, United Kingdom). Proteins were eluted with a linear gradient of NaCl (0–1.0 M) in 50 mM Tris–HCl (pH 7.5) at a flow rate of 2.0 mL · min^{-1}. Fractions with PEPCK protein were collected and concentrated using Amicon Ultra centrifugal filter unit (MWCO 10 K). Proteins were then applied to a gel filtration column, Superdex 200 Increase 10/300 GL (GE Healthcare), with a mobile phase of 50 mM Tris–HCl (pH 7.5) with 0.15 M NaCl and 10% glycerol (v/v) at a flow rate of 0.5 mL · min^{-1}. Relevant fractions were concentrated using Amicon Ultra centrifugal filter unit (MWCO 10 K). Protein concentrations were determined with the Protein Assay System (Bio-Rad, Hercules, CA, United States) using bovine serum albumin (Thermo Fisher Scientific, Waltham, MA, United States) as a standard. The homogeneity of PEPCK recombinant proteins was analyzed by sodium dodecyl sulfate-polyacrylamide gel electrophoresis (SDS-PAGE). Gels were stained with Coomassie Brilliant Blue.

Oligomerization analyses of the recombinant PEPCK proteins after purification were performed by gel filtration chromatography using the same column (Superdex 200 Increase 10/300 GL) and elution buffer as described above. The absorbance derived from protein was monitored at 280 nm. Blue Dextran 2000 was used to determine the void volume (V_0), while standard proteins (ribonuclease A: 13.7 kDa, carbonic anhydrase: 29 kDa, ovalbumin: 43 kDa, conalbumin: 75 kDa, aldolase: 158 kDa, and ferritin: 440 kDa) of Gel Filtration Calibration Kits (GE Healthcare) were utilized to prepare a calibration curve (Figure S4a). The calibration curve of partition coefficient (K_{av}) versus log molecular weight (Log_{Mr}) was plotted (Figure S4b). The K_{av} values were calculated using Equation 1, where V_0 is column void volume, V_e is protein elution volume, and V_c is the geometric column volume (24 mL).

$$K_{av} = \frac{V_e - V_0}{V_c - V_0} \quad (1)$$

Enzyme assays

Unless mentioned otherwise, PEPCK activities were assayed by measuring the oxidation of NADH at 340 nm. In the direction of carboxylation, the generated OAA was quantified by coupling with malate dehydrogenase (MDH; Sigma, Darmstadt, Germany). The carboxylation mixture (250 μL) contained 50 mM MES (pH 5.5 for *Es*-PEPCK) or HEPES (pH 6.0 for *Sl*-PEPCK; pH 6.5 for *Sj*-, *Sh*-, and *Io*-PEPCK) buffer, 50 mM $NaHCO_3$, 16 mM PEP, 2 mM ADP, 2 mM $MgCl_2$, 2 mM $MnCl_2$, 1 mM dithiothreitol (DTT), 0.15 mM NADH, 10 U MDH, and PEPCK recombinant protein. In the direction of decarboxylation, PEP generation was quantified by coupling with pyruvate kinase (PK; Sigma) and lactate dehydrogenase (LDH). The decarboxylation mixture (250 μL) contained 50 mM Tris–HCl buffer (pH 7.5), 4 mM OAA, 2 mM ATP, 2 mM $MgCl_2$, 2 mM $MnCl_2$, 1 mM DTT, 0.2 mM ADP, 0.2 mM NADH, 5 U LDH, 4 U PK, and PEPCK recombinant protein. An OAA solution was prepared just before use. Reaction mixtures without PEPCK protein were set as the controls. After a preincubation for 2 min, the reactions were started by adding ADP (for carboxylation) or OAA (for decarboxylation). The reactions were carried out at 25°C. Absorbance at 340 nm (0–3 min) was continuously monitored using a UV-1600 spectrophotometer (Shimadzu, Kyoto, Japan). The assays were performed in triplicate.

To examine the preference toward ADP and GDP, the reaction mixture (250 μL) contained 50 mM HEPES buffer (pH 6.5), 50 mM $NaHCO_3$, 8 mM PEP, 2 mM ADP or GDP, 2 mM $MgCl_2$, 2 mM $MnCl_2$, 0.15 mM NADH, 10 U MDH, and PEPCK recombinant protein.

To examine the preference toward different divalent cations, the reaction mixture (250 μL) contained 50 mM HEPES buffer (pH 6.5), 50 mM $NaHCO_3$, 8 mM PEP, 2 mM ADP, 2 mM $MgCl_2$, 2 mM divalent cation ($MnCl_2$, $CoCl_2$, $NiCl_2$, $CaCl_2$, $ZnSO_4$, $CuCl_2$, and $SrCl_2$) with or without 2 mM $MgCl_2$, 0.15 mM NADH, 10 U MDH, and PEPCK recombinant protein.

Determination of optimum pH for PEPCK recombinant proteins

The effects of pH on the decarboxylation and carboxylation reactions were examined using various buffers: sodium acetate buffer (pH 4.5–5.5), MES buffer (pH 5.5–6.5), HEPES buffer (pH 6.5–7.5), and Tris–HCl buffer (pH 7.5–9.0). We considered that the activities of MDH (for the carboxylation measurement), as well as LDH and PK (for the decarboxylation measurement), could be affected by differences in pH, resulting in inaccuracies of the data obtained via the spectrophotometric method. We thus directly quantified the production of ATP (carboxylation) and ADP (decarboxylation) with high-performance liquid chromatography (HPLC; LC-2050C 3D, Shimadzu) to measure PEPCK activities. The reaction mixture for carboxylation (50 μL) contained 50 mM buffer (pH 4.5–8.5), 50 mM $NaHCO_3$, 2 mM PEP, 1 mM ADP, 2 mM $MgCl_2$, 1 mM $MnCl_2$, 1 mM DTT, and 0.8 μg · mL^{-1} PEPCK protein. The reaction mixture for decarboxylation (50 μL) contained 50 mM buffer (pH 5.5–9.0), 2 mM OAA, 1 mM ATP, 2 mM $MgCl_2$, 1 mM $MnCl_2$, and 0.8 μg · mL^{-1} PEPCK protein. Mixtures without PEPCK protein were set as controls. After preincubation at 25°C for 2 min, reactions were started by adding OAA (decarboxylation) or PEP (carboxylation). After a 3-min incubation, reactions were stopped by rapid cooling on ice and the addition of 1 M HCl or NaOH for 5 min. After neutralization, proteins in the reaction mixtures were removed by ultrafiltration using Amicon Ultra centrifugal filter units (MWCO 3 K). Assays were performed in triplicate. The generated ADP (decarboxylation) or ATP (carboxylation) was quantified by HPLC.

The analysis of HPLC was carried out with a COSMOSIL $5C_{18}$-PAQ column (4.6 mm × 250 mm, 5 μm particle size). The generated ADP (decarboxylation) or ATP (carboxylation) was quantified as follows. The mobile phase consisted of solvent A (20 mM potassium phosphate buffer with 5 mM tetrabutylammonium hydrogen sulfate, pH 6.4) and solvent B (acetonitrile). A gradient of 0%–45% solvent B was applied from 0 to 15 min, followed by a 1-min maintenance period, then the proportion was returned back to 0% solvent B, and the column was re-equilibrated for 4 min. A flow rate of 0.7 mL · min^{-1} was maintained throughout the procedure. Absorbance at 259 nm was monitored by a UV detector.

Kinetic analysis

Kinetic analyses of the PEPCK reactions were carried out as follows. For the carboxylation reaction, reaction mixtures consisted of 50 mM MES (pH 5.5 for *Es*-PEPCK) or HEPES (pH 6.0 for *Sl*-PEPCK; pH 6.5 for *Sj*-, *Sh*-, and *Io*-PEPCK) buffer, 50 mM $NaHCO_3$, 16 mM PEP, 2 mM ADP, 2 mM $MgCl_2$, 2 mM $MnCl_2$, 1 mM DTT, 0.15 mM NADH, 10 U MDH, and 0.4–0.8 μg · mL^{-1} PEPCK recombinant protein. When varying the concentration of a given substrate, the concentrations of other substrates were fixed at the concentrations given above. The concentration range of the evaluated substrates was ADP (0.025 mM to 5 mM) and PEP (0.05 mM to 8 or 12 mM). For the kinetic analysis of PEPCK toward bicarbonate, *Io*-PEPCK protein was used. The reaction mixture was composed of 50 mM HEPES (pH 6.5) buffer, 16 mM PEP, 2 mM ADP, 2 mM $MgCl_2$, 2 mM $MnCl_2$, 1 mM DTT, 0.15 mM NADH, 10 U MDH, 0.4 μg · mL^{-1} *Io*-PEPCK, and various concentrations of $NaHCO_3$ (0.5 mM to 50 mM) added from a stock solution (5, 50, or 500 mM) prepared immediately prior to the experiments. The presence of bicarbonate

from atmospheric carbon dioxide was negligible, with activity less than 0.1 μmol · min^{-1} · mg^{-1}. The kinetic parameters of the decarboxylation reaction catalyzed by *Io*-PEPCK toward OAA and ATP were measured. Activities with varying concentrations of OAA (0.025 mM to 5 mM) were measured by coupling with PK/LDH. Activities with varying concentrations of ATP (0.01 mM to 2 mM) were measured by determining the generated ADP via HPLC, as PK would regenerate ATP from ADP produced by PEPCK and thus affect the determination, particularly at low concentrations of ATP. The decarboxylation mixture (250 μL) for kinetic examination of OAA was composed of 50 mM Tris–HCl buffer (pH 7.5), 2 mM ATP, 2 mM $MgCl_2$, 2 mM $MnCl_2$, 1 mM DTT, 0.2 mM ADP, 0.2 mM NADH, 5 U LDH, 4 U PK, 0.4 μg · mL^{-1} *Io*-PEPCK recombinant protein, and various concentrations of OAA. The decarboxylation mixture (50 μL) for kinetic examination of ATP was composed of 50 mM Tris–HCl buffer (pH 7.5), 4 mM OAA, 2 mM $MgCl_2$, 2 mM $MnCl_2$, 1 mM DTT, 0.2 μg · mL^{-1} *Io*-PEPCK recombinant protein, and various concentrations of ATP. All assays were performed in triplicate. The Michaelis–Menten equation was fit to the data using software Igor Pro, version 6.03AJ (WaveMetrics, Portland, OR, United States).

Effect of various metabolites on *Io*-PEPCK activity

To avoid any unexpected effects of the examined metabolites, such as pyruvate or malate, on LDH/PK or MDH, the effects of various metabolites on *Io*-PEPCK were analyzed by measuring the generation of ATP (carboxylation) or ADP (decarboxylation) via HPLC. The following metabolites were examined: amino acids alanine, arginine, aspartate, glutamate, glycine, and phenylalanine; TCA cycle intermediates citrate, succinate, and malate; glycolysis intermediates pyruvate, glucose 6-phosphate, fructose 1,6-bisphosphate, and 3-phosphoglycerate; and acetate. The carboxylation mixture (50 μL) contained 50 mM HEPES buffer (pH 6.5), 50 mM $NaHCO_3$, 16 mM PEP, 2 mM ADP, 2 mM $MgCl_2$, 2 mM $MnCl_2$, 1 mM DTT, 0.2 μg · mL^{-1} *Io*-PEPCK recombinant protein, and 5 mM metabolite. The decarboxylation mixture (50 μL) contained 50 mM Tris–HCl buffer (pH 7.5), 4 mM OAA, 2 mM ATP, 2 mM $MgCl_2$, 2 mM $MnCl_2$, 1 mM DTT, 0.2 μg · mL^{-1} *Io*-PEPCK recombinant protein, and 5 mM metabolite. All assays were performed in triplicate.

To study the effects of ATP on the carboxylation activity of *Io*-PEPCK, the concentration of ADP was fixed at 2 mM, while the concentrations of ATP ranged from 0 to 4 mM. To analyze inhibition by ATP, carboxylation activities of *Io*-PEPCK toward various ADP concentrations (0.1, 0.2, 0.4, 0.8, 1, 1.5, 2, 3, and 4 mM) with 1, 2, 3, or 4 mM ATP were examined by coupling with MDH. The carboxylation activity with ADP but without ATP was set as the control. The carboxylation activity was measured by measuring the oxidation of NADH. All assays were performed in triplicate.

Preparation of cell-free extract and activity measurement

Extraction of total soluble proteins from the plants of brown alga *Ishige okamurae* was carried out based on the method previously reported (Capó-Bauçà et al., 2023). Pieces of *I. okamurae* (~4 g fresh weight) were frozen and ground to a fine powder with liquid nitrogen and alpha-alumina powder in a prechilled mortar. The powder was homogenized with 12 mL of ice-cold extraction buffer consisting of 100 mM Bicine (pH 8.0), 1 mM ethylenediaminetetraacetic acid, 10 mM DTT, 100 mM β-mercaptoethanol, 2% plant protease inhibitor cocktail (Merck, Burlington, MA, United States), 4 mM PMSF, and 0.5% Triton X-100. Polyvinylpolypyrrolidone (0.6 g) was added to the mixture to reduce viscosity, followed by stirring with an ice-cold spatula. After centrifugation (4°C, 15000 x *g*, 2 min), the supernatant was concentrated using an Amicon Ultra centrifugal filter unit (MWCO 10 K) and then loaded onto a PD-10 column (GE Healthcare) to remove the metabolites from the cell extract using a buffer consisting of 50 mM Tris–HCl (pH 7.5), 0.15 M NaCl, 1% plant protease inhibitor cocktail, 4 mM PMSF, and 10% glycerol (v/v). The total soluble protein content was determined using the method described above.

The specific PEPCK (carboxylation and decarboxylation) and PEPC activities of total soluble proteins were examined by measuring the oxidation of NADH. The mixture (250 μL) to measure PEPCK carboxylation activity contained 50 mM HEPES buffer (pH 6.5), 50 mM $NaHCO_3$, 16 mM PEP, 2 mM ADP, 2 mM $MgCl_2$, 2 mM $MnCl_2$, 1 mM DTT, 0.15 mM NADH, 10 U MDH, and 4 μg · mL^{-1} total protein. The mixture (250 μL) to measure decarboxylation activity contained 50 mM Tris–HCl buffer (pH 7.5), 1 mM OAA, 2 mM ATP, 2 mM $MgCl_2$, 2 mM $MnCl_2$, 1 mM DTT, 0.2 mM ADP, 0.2 mM NADH, 5 U LDH, 4 U PK, and 4 μg · mL^{-1} total protein. The concentration of OAA for the decarboxylation measurement was lowered to 1 mM to limit the effects of nonenzymatic degradation of OAA. The PEPC activity of total soluble proteins was measured using a reaction mixture containing 50 mM Tris–HCl buffer (pH 8.0), 50 mM $NaHCO_3$, 16 mM PEP, 2 mM $MgCl_2$, 1 mM DTT, 0.15 mM NADH, 10 U MDH, and 8 μg · mL^{-1} total protein. All assays were performed in triplicate.

Bioinformatic analysis of PEPCK sequences

The phylogenetic tree of PEPCKs was constructed with MEGA11 (Tamura et al., 2021) using the maximum

likelihood method and JTT matrix-based model (Jones et al., 1992) with default parameters. Amino acid sequence alignments were carried out with ClusterX2 (Larkin et al., 2007) and colored with Web server ESPript 3.0 (http://espript.ibcp.fr/ESPript/ESPript/; Robert & Gouet, 2014). The subcellular localizations, signal/transit peptide sequences, and potential cleavage sites of these PEPCK were predicted by TargetP-2.0 (https://services.healthtech.dtu.dk/services/TargetP-2.0/; Almagro et al., 2019) and DeepLoc 2.0 (https://services.healthtech.dtu.dk/services/DeepLoc-2.0/; Thumuluri et al., 2022).

RESULTS

Primary structure analysis of five PEPCKs from brown macroalgae

We used the PEPCK (*Sj*-PEPCK) sequence from *Saccharina japonica* as the query to perform a Blast search with the NCBI database. At the time of this study, the number of available genome sequences or transcriptome data of brown algae was still limited (<20). An alignment of the sequences retrieved from the search is shown in Figure S5a. The result of a phylogenetic analysis showed that the PEPCKs from brown algae were separated into several subgroups (Figure S5b). As we wanted to obtain a broad picture of the properties of PEPCK from brown algae, we selected multiple proteins for analyses. We selected the putative PEPCKs from *Ectocarpus siliculosus* (*Es*-PEPCK), *Ishige okamurae* (*Io*-PEPCK), *Sargassum horneri* (*Sh*-PEPCK), and *Scytosiphon lomentaria* (*Sl*-PEPCK) in addition to *Sj*-PEPCK. Although the five putative PEPCKs were 77%–87% identical to one another, the proteins represented different subgroups of the PEPCKs in the phylogenetic tree (Figure S5b). The proteins from brown algae shared 46%–49% identities with their counterpart from *Escherichia coli* (*Eco*-PEPCK). Each species harbored only a single sequence with homology to previously reported PEPCKs.

The ATP and GTP-dependent PEPCKs harbored several essential motifs, including the PEPCK-specific domain, kinase-1a (P-loop) and kinase-2 domains, and an adenine or a guanine binding site, which are responsible for the association with PEP/OAA, phosphate-binding, Mg^{2+} binding, and adenine or guanine binding, respectively (Dunten et al., 2002; Matte et al., 1996; Matte et al., 1997; Tari et al., 1996; Tari et al., 1997). We aligned the sequences of the five algal PEPCKs with other experimentally examined ATP-dependent PEPCKs from various organisms, including bacteria, yeast, plants, and green alga (Figure S6). All five putative brown algal PEPCKs possessed the conserved binding motifs. In addition, the five proteins harbored the motifs for ribose and adenine binding, suggesting that they were ATP-dependent PEPCKs. All five algal proteins harbored the key residues that constitute the active site in *Eco*-PEPCK (Delbaere et al., 2004; Sudom et al., 2001; Sudom et al., 2003).

Predictions using TargetP and DeepLoc (Almagro et al., 2019; Thumuluri et al., 2022) on the five PEPCKs suggested that they localized in the mitochondrion or chloroplast (Table S2). Their signal peptides (30–47 aa length, from the initial Met) and the predicted cleavage sites are shown in Table S2.

Expression and purification of the recombinant PEPCK proteins

The five putative PEPCK genes were synthesized and individually modified to introduce a 6 x His tag sequence at their N-termini. Sequences corresponding to their predicted signal peptides (about 90–141 bps) were removed, and the resulting truncated genes were expressed in *Escherichia coli* BL21-CodonPlus(DE3)-RIL (Figure S3). After adding isopropyl β-D-1-thiogalactopyranoside (IPTG), cells were cultivated at 16°C to reduce the formation of inclusion bodies. The His-tagged recombinant proteins were purified using a nickel chelate affinity column, followed by anion-exchange and gel-filtration chromatography. The apparent homogeneities of the recombinant proteins were examined by SDS-PAGE. The obtained bands displayed molecular masses that corresponded well to their theoretical molecular masses (*Es*-: 59.2 kDa, *Io*-: 59.7 kDa, *Sh*-: 63.3 kDa, *Sj*-: 59.3 kDa, and *Sl*-PEPCK: 59.3 kDa; Figure S7).

Oligomerization analysis of the putative PEPCK recombinant proteins was performed by gel-filtration chromatography (Figure S4c). *Es*-, *Io*-, *Sh*-, *Sj*-, and *Sl*-PEPCK were individually eluted at 14.21, 14.26, 13.77, 14.24, and 14.11 mL, corresponding to calculated molecular masses of 59.2, 57.9, 72.0, 58.4, and 61.9 kDa, respectively. These values were comparable to the theoretical molecular masses of the monomers, suggesting that the putative PEPCKs are monomeric proteins.

Substrates recognized by the PEPCKs from brown algae

The PEPCKs from brown algae were predicted to be ATP-dependent based on their amino acid sequences. To confirm this, the carboxylation activity of the five PEPCKs was examined using ADP or GDP (Figure S8). The activity levels of *Es*-, *Io*-, *Sh*-, *Sj*-, and *Sl*-PEPCK with ADP were significantly higher (23-, 40-, 47-, 30-, and 42-fold, respectively) than those with GDP, confirming that these proteins are ATP-dependent PEPCKs.

Previously known PEPCKs are metal-dependent enzymes, which often utilize Mg^{2+} and a second metal ion such as Mn^{2+}. We first examined the effect of adding various divalent metal cations on the five PEPCKs in the presence of 2 mM Mg^{2+} (Figure S9). In the presence of Mg^{2+}, the addition of Mn^{2+} resulted in the highest carboxylation activity of the PEPCK proteins, with activities reaching more than 48-fold over that observed in the presence of Mg^{2+} alone (*Io*-PEPCK). A dramatic increase in activity was also observed with Co^{2+} in the presence of Mg^{2+}. The addition of Ni^{2+} had little effect on activity, while Ca^{2+}, Zn^{2+}, Cu^{2+}, and Sr^{2+} resulted in a decrease in activity. When only a single divalent cation was available, in all five PEPCKs, Mn^{2+} alone supported carboxylation activities as high as or even higher than those observed with Mg^{2+} and Mn^{2+}. Co^{2+} alone also supported high activity, although levels were lower than those observed with Mn^{2+} alone. It has been reported that the concentration of Mn^{2+} in algae cells is low, much lower than that of Mg^{2+}. Concentrations of Mg^{2+} have been reported to be 280- to 1900-fold higher than those of Mn^{2+} (Wahbeh et al., 1985). Therefore, the possibilities of the PEPCK enzymes in algal cells using Mn^{2+} alone were considered extremely low, and further enzyme analyses were carried out in the presence of both Mg^{2+} and Mn^{2+}.

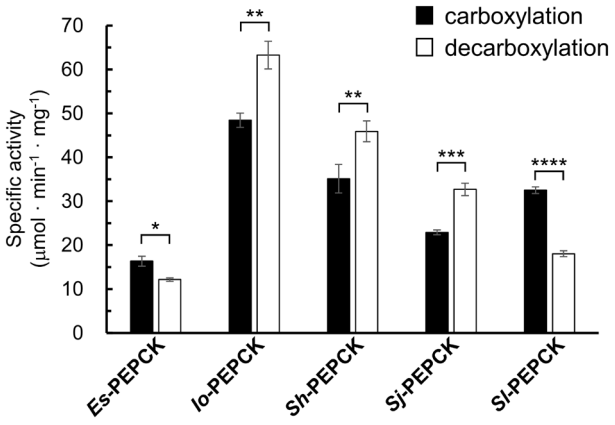

FIGURE 2 Specific activity of recombinant PEPCK proteins from various brown algae. The carboxylation activity is indicated with black bars, and the reaction mixture contained 50 mM MES (pH 5.5 for PEPCK from *E. siliculosus* [*Es*-PEPCK]) or HEPES (pH 6.0 for *S. lomentaria* [*Sl*-PEPCK]; pH 6.5 for PEPCKs from *S. japonica* [*Sj*-PEPCK], *S. horneri* [*Sh*-PEPCK], and *I. okamurae* [*Io*-PEPCK]) buffer, 2 mM ADP, 16 mM PEP, and 50 mM $NaHCO_3$. The decarboxylation activity is indicated with white bars and the reaction mixture contained 50 mM Tris–HCl buffer (pH 7.5), 2 mM ATP and 4 mM OAA. *Es*: *Ectocarpus siliculosus*, *Io*: *Ishige okamurae*, *Sh*: *Sargassum horneri*, *Sj*: *Saccharina japonica*, *Sl*: *Scytosiphon lomentaria*. The data represent the average of three independent experiments and are shown with the *SD* values. $10^{-2} < p \leq 0.05$: *; $10^{-3} < p \leq 10^{-2}$: **; $10^{-4} < p \leq 10^{-3}$: ***; $10^{-7} < p \leq 10^{-6}$: ****.

Specific activity measurement and kinetic analysis of PEPCK recombinant proteins

The effect of pH on PEPCK activity was examined in both the carboxylation (pH 4.5–8.5) and decarboxylation (5 to 9) directions. *Es*- and *Sl*-PEPCK displayed their highest carboxylation activity at pH 5.5 and 6.0, respectively, while *Io*-, *Sh*-, and *Sj*-PEPCK preferred pH 6.5 (Figure S10a). All five enzymes showed maximum decarboxylation activity at pH 7.5 (Figure S10b).

The specific carboxylation and decarboxylation activities of the five PEPCKs were measured under optimal reaction conditions. Although the five PEPCKs shared high identities, they displayed differences in activity (Figure 2). *Io*-PEPCK displayed the highest activities in both the carboxylation and decarboxylation directions, with specific activities of 48.4 ± 1.6 and 63.3 ± 3.2 μmol · min^{-1} · mg^{-1}, respectively. In contrast, *Es*-PEPCK showed the lowest activities (16.4 ± 1.1 and 12.2 ± 0.4 μmol · min^{-1} · mg^{-1} in carboxylation and decarboxylation, respectively).

We next carried out a kinetic examination of the five proteins in the direction of carboxylation. *Io*-PEPCK displayed the highest k_{cat}/K_m values for PEP and ADP, and there was an approximate threefold difference in corresponding k_{cat}/K_m values among the five enzymes (Table 1, Figures 3 and S11), mainly due to differences in k_{cat} values. For further analysis, we selected *Io*-PEPCK, which displayed the highest k_{cat}/K_m values for PEP and ADP among the five enzymes. When activity was measured with varying concentrations of bicarbonate, the activity followed Michaelis–Menten kinetics, and a V_{max} value comparable with those observed with varying concentrations of ADP and PEP was obtained. We also carried out a kinetic examination in the direction of decarboxylation using *Io*-PEPCK. The k_{cat}/K_m values were slightly higher for the decarboxylation reaction compared to the carboxylation reaction (Table 1), consistent with previous studies on ATP-dependent PEPCKs.

Effect of metabolites on *Io*-PEPCK activity

To explore the potential modulation of PEPCK in brown algae, we examined the response of *Io*-PEPCK to various metabolites, including those related to C3/C4 conversion (pyruvate, malate, succinate, alanine, aspartate) and those that have been examined on PEPCK activity in other organisms (acetate, arginine, glycine, phenylalanine, glucose 6-phosphate [G6P], fructose 1,6-bisphosphate [FBP], 3-phosphoglycerate [3-PGA], citrate, glutamate; Figure 4). We did not observe dramatic effects of these compounds in either the carboxylation or decarboxylation activities. We did observe a slight tendency suggesting that the presence of citrate and malate might induce decarboxylation, as they enhanced the decarboxylation activity (citrate by 25%, malate by 16%) while inhibiting the carboxylation activity by 20% (Figure 4).

TABLE 1 Kinetic parameters of PEPCKs from brown algae.

Enzymes	Substrates	V_{max} (μmol · min^{-1} · mg^{-1})	K_m (mM)	k_{cat} (s^{-1})	k_{cat}/K_m ($M^{-1} \cdot s^{-1}$)
Io-PEPCK	ADP	51.9 ± 1.0	0.11 ± 0.01	51.6 ± 1.0	4.7×10^5
	PEP	56.4 ± 1.5	0.76 ± 0.07	56.1 ± 1.5	7.4×10^4
	$NaHCO_3$	61.6 ± 1.4	6.69 ± 0.44	61.3 ± 1.4	9.2×10^3
	ATP	75.8 ± 1.6	0.07 ± 0.01	75.4 ± 1.6	1.1×10^6
	OAA	63.8 ± 0.9	0.18 ± 0.01	63.5 ± 0.9	3.5×10^5
Sh-PEPCK	ADP	37.5 ± 0.6	0.14 ± 0.01	39.5 ± 0.6	2.8×10^5
	PEP	39.2 ± 1.1	0.70 ± 0.07	41.4 ± 1.2	5.9×10^4
Sl-PEPCK	ADP	34.3 ± 0.4	0.10 ± 0.01	33.9 ± 0.4	3.4×10^5
	PEP	32.0 ± 1.1	1.33 ± 0.15	31.7 ± 1.0	2.4×10^4
Sj-PEPCK	ADP	23.6 ± 0.4	0.08 ± 0.01	23.3 ± 0.4	2.9×10^5
	PEP	23.0 ± 0.9	1.10 ± 0.13	22.7 ± 0.9	2.1×10^4
Es-PEPCK	ADP	17.8 ± 0.2	0.13 ± 0.01	17.6 ± 0.2	1.4×10^5
	PEP	16.8 ± 0.3	0.62 ± 0.05	16.5 ± 0.3	2.7×10^4

Note: PEPCKs from *I. okamurae* (*Io*-PEPCK), *S. horneri* (*Sh*-PEPCK), *S. lomentaria* (*Sl*-PEPCK), *S. japonica* (*Sj*-PEPCK), *E. siliculosus* (*Es*-PEPCK) were analyzed.

We also examined the inhibition of the carboxylation activity of *Io*-PEPCK by ATP, which has been reported in the PEPCKs from several organisms. In the presence of 2 mM ADP, 16 mM PEP, and 50 mM $NaHCO_3$, 0.2–4 mM of ATP were added to the carboxylation reaction mixture (Figure 5a). A decrease in activity was observed at ATP concentrations above 1 mM. When ATP was present at 4 mM, the decrease in carboxylation activity was nearly 90%. We thus carried out carboxylating activity measurements with various ADP concentrations (0.1–4 mM) in the presence of 1, 2, 3, or 4 mM ATP (as an inhibitor; Figure 5b). We considered that contributions of the reverse reaction to our results were limited, as accumulation of the product OAA was prevented by the coupling enzyme malate dehydrogenase, which was present in excess. We observed that the data fit well to a mixed-type inhibition model (Figure S12) whose equation is indicated in Equation 2.

$$v = \frac{V_{max}[S]}{K_s\left(1 + \frac{[P]}{K_p}\right) + [S]\left(1 + \frac{[P]}{\alpha K_p}\right)} \quad (2)$$

Concentrations of the substrate ADP and the inhibitor ATP are designated [S] and [P], respectively. K_s and K_p are the dissociation constants for the substrate ADP and the product inhibitor ATP, respectively. The change of dissociation constant between enzyme-ADP complex and ATP compared to that between enzyme and ATP was designated as a factor of α. We assigned V_{max} and K_s values of 51.9 μmol · min^{-1} · mg^{-1} and 0.11 mM, respectively, which were calculated from the analysis of the reaction in the absence of ATP. Equation 2 fit well to our data with various concentrations of ATP, and the constants K_p and α were calculated as 0.095 ± 0.021 mM and 28.0 ± 7.7, respectively. As α was greater than 1, the binding of ATP occurred more toward the vacant enzyme than toward the enzyme-ADP complex. Our result suggests that allosteric binding of ATP to *Io*-PEPCK causes a mixed-type inhibition against the carboxylation reaction.

Measurement of PEPCK and PEPC activities from cell extract of *Ishige okamurae*

In order to explore the function(s) of PEPCK in brown algae, we extracted the total soluble proteins from the brown alga *Ishige okamurae*, and measured PEPCK and PEPC activities. The PEPCK specific activity of total soluble proteins was 1.04 ± 0.10 μmol · min^{-1} · mg^{-1} in the direction of carboxylation and 1.11 ± 0.07 μmol · min^{-1} · mg^{-1} in that of decarboxylation. The level of PEPCK carboxylation activity was 3.5-fold higher than that observed in cell extracts of *Ascophyllum nodosum* (0.3 μmol · min^{-1} · mg^{-1}), a species of brown algae also considered to utilize PEPCK instead of PEPC in C_4-like metabolism (Johnston & Raven, 1989). In terms of PEPC activity, the activity in cell extracts of *I. okamurae* was 0.09 ± 0.00 μmol · min^{-1} · mg^{-1}, corresponding to only 9% of PEPCK carboxylating activity (Figure 6). This result suggests that PEPCK rather than PEPC dominates the carboxylation in *I. okamurae*, which is consistent with previous studies on other brown algae.

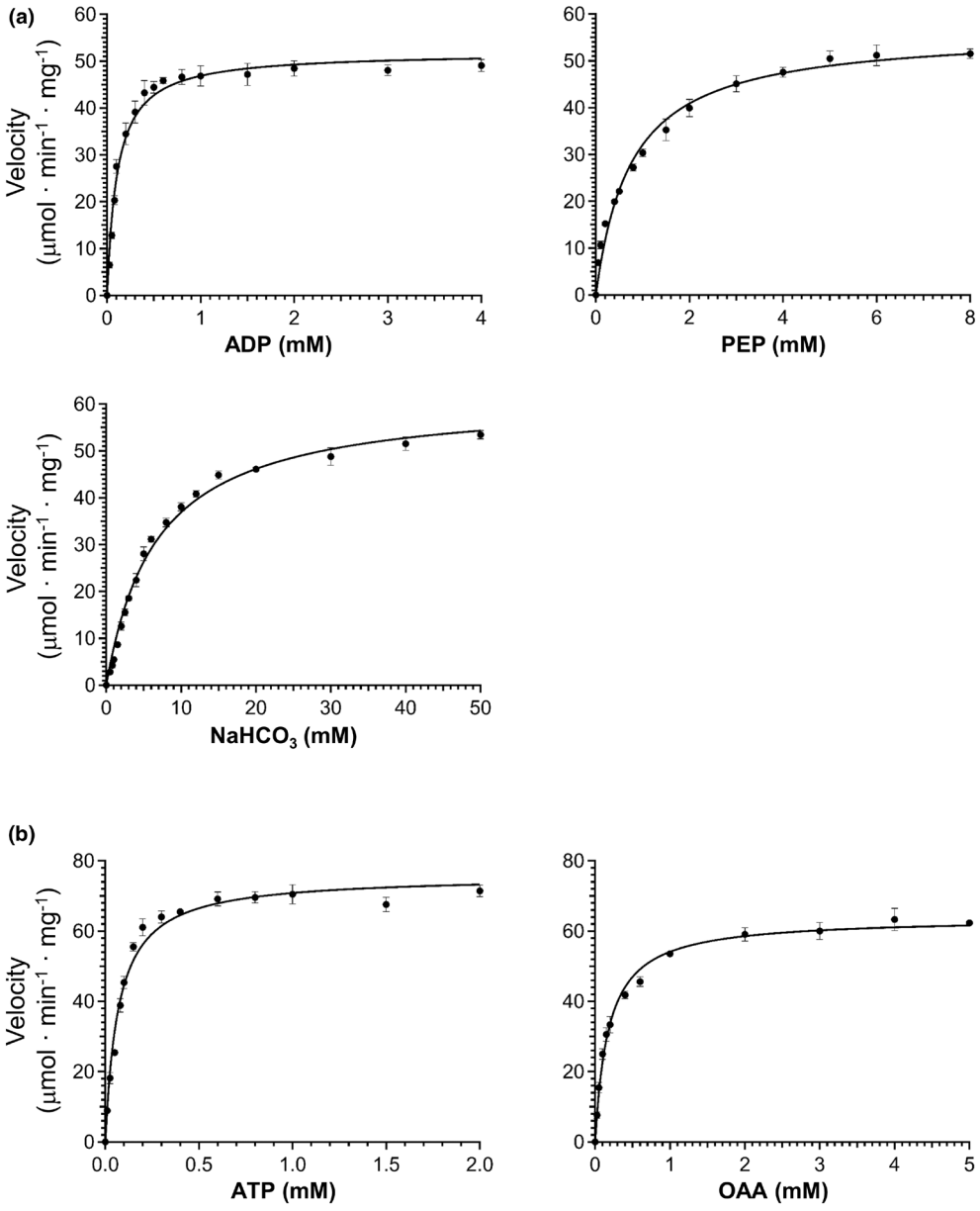

FIGURE 3 Kinetic analysis of the *Io*-PEPCK (PEPCK from *I. okamurae*) reaction in the carboxylation (a) and decarboxylation (b) directions. The effects of ADP, PEP, and $NaHCO_3$ concentrations on the carboxylation activity and those of ATP and OAA concentrations on the decarboxylation activity were examined. When varying the concentration of a given substrate, the other substrates were fixed at the following concentrations: 2 mM ADP, 16 mM PEP, and 50 mM $NaHCO_3$ in carboxylation; 2 mM ATP and 4 mM OAA in decarboxylation.

DISCUSSION

Brown algae are presumed to employ a C_4-like pathway to concentrate CO_2 for carbon fixation by RuBisCO (Shao et al., 2019). However, the enzymes, metabolites, and pathways involved in CCMs in brown algae are still poorly understood. The biochemical properties of the enzymes involved and their subcellular localization must be elucidated to better understand the CO_2-fixing mechanism in brown algae. This study presented the enzymatic properties of purified PEPCKs from multiple brown macroalgae. The results provided enzymatic properties that can be presumed to be widely shared among PEPCKs from brown algae.

Although the identities among the five enzymes were higher than 77%, we observed differences in their carboxylation activities, most prominently in turnover numbers (k_{cat}). There was an approximate threefold difference between the highest (*Io*-PEPCK) and the lowest (*Es*-PEPCK) activities. Intriguingly, *Io*-, *Sh*-, and *Sj*-PEPCKs displayed higher decarboxylation activity than carboxylation activity, whereas *Es*- and *Sl*-PEPCKs displayed higher carboxylation activities (Figure 2). The mechanistic reason for this is

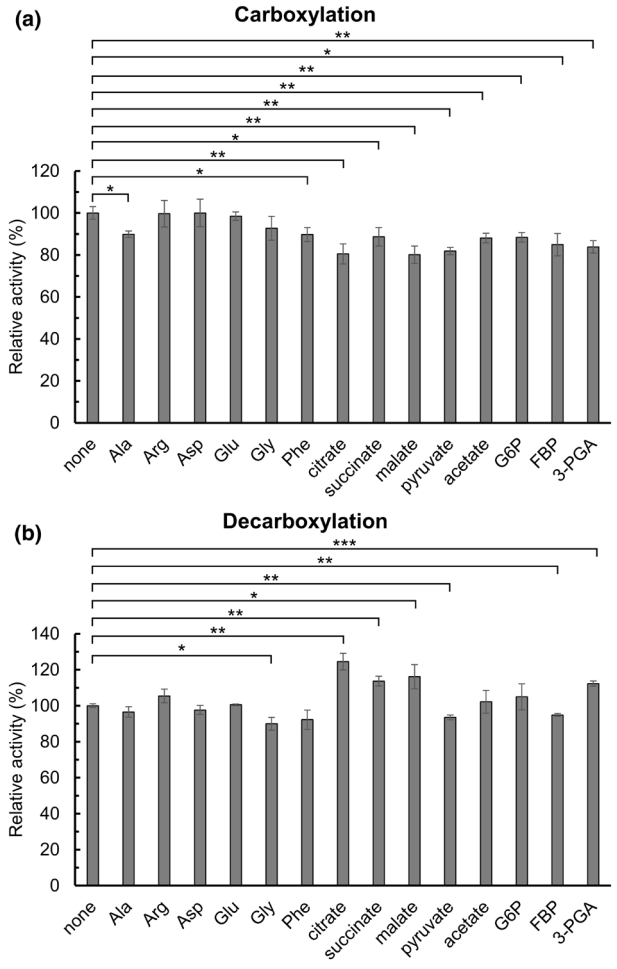

FIGURE 4 Effect of various metabolites on carboxylation (a) and decarboxylation (b) activity of *Io*-PEPCK (PEPCK from *I. okamurae*) protein. The effects of various metabolites at a concentration of 5 mM on the activity of *Io*-PEPCK. The metabolites were: Alanine (Ala), arginine (Arg), aspartate (Asp), glutamate (Glu), glycine (Gly), phenylalanine (Phe), citrate, succinate, malate, pyruvate, acetate, glucose 6-phosphate (G6P), fructose 1,6-bisphosphate (FBP), and 3-phosphoglycerate (3-PGA). Activities in the absence of metabolites (none) were set as the controls. The data represent the average of three independent experiments and are shown with the *SD* values. $10^{-2} < p \leq 0.05$: *; $10^{-3} < p \leq 10^{-2}$: **; $10^{-4} < p \leq 10^{-3}$: ***.

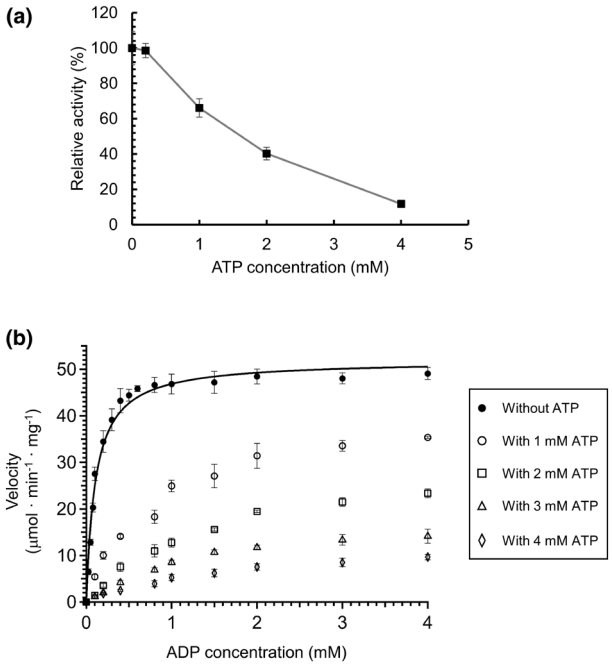

FIGURE 5 Effect of ATP on the carboxylation activity of *Io*-PEPCK (PEPCK from *I. okamurae*). (a) The relative carboxylation activity of *Io*-PEPCK in the presence of various ATP concentrations (0, 0.2, 1, 2, and 4 mM) with 2 mM ADP. (b) The effect of ATP on carboxylation activity of *Io*-PEPCK. The carboxylation velocity of *Io*-PEPCK was measured using various concentrations of ADP (substrate) in the absence or presence (1, 2, 3, or 4 mM) of ATP.

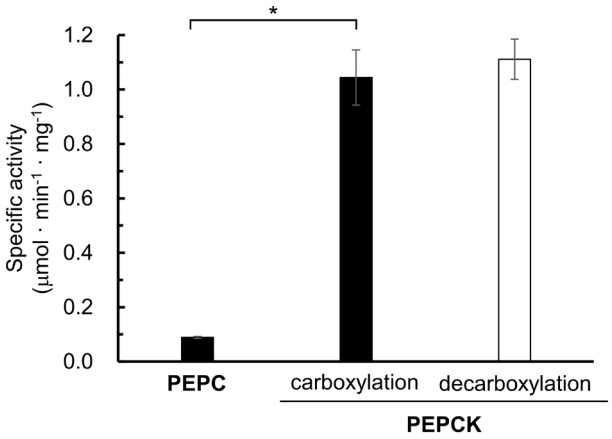

FIGURE 6 PEPC and PEPCK activities in *Ishige okamurae* cell extract. PEPC and PEPCK activities in cell-free extracts of *I. okamurae* were examined. Two micrograms of cell-free extract was used to measure PEPC activity and 1 μg was used for PEPCK measurements. The data represent the average of three independent experiments and are shown with the *SD* values. $10^{-3} < p \leq 10^{-2}$: *.

unknown, but *Es*- and *Sl*-PEPCKs are structurally related to one another (Figure S5). In addition, this may be related to the optimal pH and the reaction conditions applied for the enzymes. In the decarboxylation reaction, all five enzymes displayed an optimal pH of 7.5, and activities were measured at this pH. In the carboxylation direction, *Io*-, *Sh*-, and *Sj*-PEPCKs displayed an optimal pH of 6.5, while those for *Es*- and *Sl*-PEPCKs were 5.5 and 6.0, respectively. Whereas PEPC utilized bicarbonate as a substrate, it has been shown that the true substrate of PEPCK in the carboxylation direction is CO_2 (Cooper et al., 1968; Miller & Lane, 1968). The concentration of CO_2, compared to that of bicarbonate, displayed dramatic increases when the pH decreased from 6.5 ($[CO_2]/[HCO_3^-] = \sim 0.71$) to 5.5 ($[CO_2]/[HCO_3^-] = \sim 7.1$), and this may have had an effect on the measured specific activity, favoring carboxylation. Overall, the activity levels of PEPCKs from brown algae were comparable to or higher than those of their counterparts from terrestrial plants and microorganisms. These included enzymes from the C_4 grass

TABLE 2 Comparison of kinetic parameters of ATP-dependent PEPCKs from different organisms.

Organism	Carboxylation					Decarboxylation		
	V_{max} (μmol · min^{-1} · mg^{-1})	K_m (mM)			$V_{max} / K_m [HCO_3^-]$	V_{max} (μmol · min^{-1} · mg^{-1})	K_m (mM)	
		ADP	PEP	HCO_3^-			ATP	OAA
Ishige okamurae (*Io*-PEPCK)	61.6	0.11	0.76	6.69	9.2	75.8	0.07	0.18
Sargassum horneri (*Sh*-PEPCK)	39.2	0.14	0.7	–	–	–	–	–
Scytosiphon lomentaria (*Sl*-PEPCK)	34.3	0.1	1.33	–	–	–	–	–
Saccharina japonica (*Sj*-PEPCK)	23.6	0.08	1.1	–	–	–	–	–
Ectocarpus siliculosus (*Es*-PEPCK)	17.8	0.13	0.62	–	–	–	–	–
Cucumis sativus (Walker et al., 1995)	48	0.027	0.34	16	3	–	0.014	0.017
Megathyrsus maximus (Burnell, 1986; Walker et al., 2002)	41.6	0.036	2.1	–	–	51	0.026	0.156
Saccharomyces cerevisiae (Andrade et al., 2010)	16	0.016	3	2	8	20	0.016	0.2
Anaerobiospirillum succiniciproducens (Podkovyrov & Zeikus, 1993)	10	0.42	0.54	17	0.6	–	2.3	1.2
Ananas comosus (Daley et al., 1977; Martin et al., 2011)	8.1	0.13	0.56	3.4	2.4	17	0.12	0.4
Chlamydomonas reinhardtii (Cre-PEPCK1, hexamer) (Torresi et al., 2023)	6	0.1	0.56	–	–	9.6	0.085	0.067
Trypanosoma cruzi (Cymeryng et al., 1995)	3.4	0.017	0.035	2.77	1.2	32	0.027	0.044
Arabidopsis thaliana (Rojas et al., 2019)	3.2	0.039	3.8	–	–	5.4	0.018	0.1
Escherichia coli (Cotelesage et al., 2007)	3	1.6	11	19	0.2	26	0.26	0.51

Megathyrsus maximus, the C_3 plants *Cucumis sativus* and *Arabidopsis thaliana*, the CAM plant *Ananas comosus*, and the bacteria *Anaerobiospirillum succiniciproducens* and *Escherichia coli* (Table S3). The number of enzymes for which $V_{max} / K_{m\,[HCO_3^-]}$ values have been determined is still limited, but that of *Io*-PEPCK was higher than those of previously studied enzymes, including that from the CAM plant *Ananas comosus* (pineapple; *Aco*-PEPCK) (Table 2).

In previously characterized ATP-dependent PEPCKs, activity in the presence of both Mg^{2+} and Mn^{2+} was higher than that in the presence of Mn^{2+} alone. It has been reported that the presence of Mg^{2+} enhances the affinity of the enzyme for Mn^{2+} (Fukuda et al., 2004; Lee et al., 1981; Tari et al., 1997). The crystal structure of the ATP-dependent PEPCK from *Escherichia coli* revealed the binding sites for Mg^{2+} and Mn^{2+} (Tari et al., 1997). Possibly correlating to the fact that Mg^{2+} is a hard Lewis acid, Mg^{2+} seems to be coordinated into an all-oxygen ligand environment, and its position is consistent with its role as a cosubstrate with ATP. In contrast, the slightly larger and softer Lewis acid Mn^{2+} is bound to a mixture of oxygen and nitrogen ligands and acts to reduce the electrostatic repulsions between the enolate of pyruvate and the γ-phosphate of ATP in the crystals (Tari et al., 1997). Intriguingly, we observed that the carboxylase activities of the PEPCKs from the five brown algae in the presence of Mn^{2+} alone were higher (13%–25%) than those with both Mg^{2+} and Mn^{2+}. As the Mg^{2+}- and Mn^{2+}-binding residues in PEPCK from *E. coli* were completely conserved in the PEPCKs from brown algae (Figure S6), the position and roles of the Mn^{2+} that replaced the Mg^{2+} in the *E. coli* enzyme are of interest.

We observed that the five PEPCKs from brown algae existed as monomers, as is the case for enzymes in *Escherichia coli* (*Eco*-PEPCK; Sudom et al., 2003) and *Anaerobiospirillum succiniciproducens*

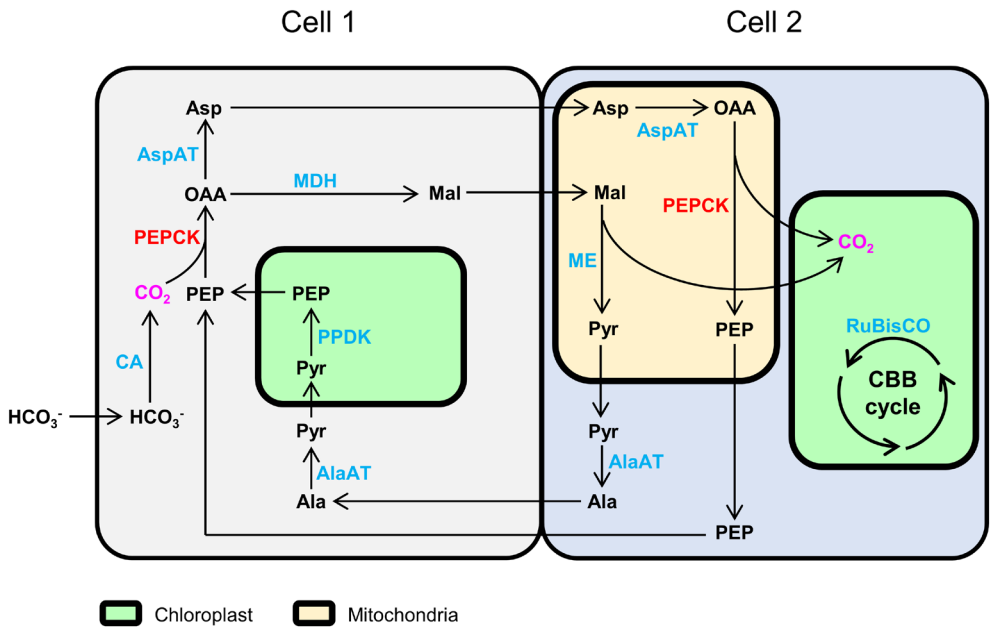

FIGURE 7 Proposed model of C_4 cycle in brown alga *Ishige okamurae*. The proposed C_4 pathway in brown algae based on this study and previous findings. In this pathway, PEPCK was proposed to replace the role of PEPC and be responsible for both fixation (in cytoplasm) and release of CO_2 (in mitochondrion). Metabolite abbreviations: Ala, alanine; Asp, aspartate; Mal, malate; OAA, oxaloacetate; PEP, phosphoenolpyruvate; Pyr, pyruvate. Enzymes: AlaAT, alanine aminotransferase; AspAT, aspartate aminotransferase; CA, carbonic anhydrase; MDH, malate dehydrogenase; ME, malic enzyme; PEPCK, PEP carboxykinase; PPDK, pyruvate orthophosphate dikinase; RuBisCO, ribulose-1,5-bisphosphate carboxylase/oxygenase.

(*Asu*-PEPCK; Podkovyrov & Zeikus, 1993). PEPCKs with other quaternary structures are known, including enzymes from the plants *Megathyrsus maximus* (hexamer; Burnell, 1986), *Arabidopsis thaliana* (hexamer; Rojas et al., 2019), and *Cucumis sativus* (tetramer; Walker et al., 1995); from *Saccharomyces cerevisiae* (tetramer; Andrade et al., 2010); from the parasite *Trypanosoma cruzi* (dimer; Trapani et al., 2001); and from the diatom *Skeletonema costatum* (dimer; Cabello-Pasini et al., 2000). Structural analysis of *T. cruzi* PEPCK (*Tcr*-PEPCK) suggested that residues in the N-terminal region (in the domain of Leu10-Gly31) played roles in the oligomerization of the protein (Figure S6; Trapani et al., 2001). However, this alone may not explain the tendency for subunit assembly, as the five PEPCKs from brown algae, as well as *Eco*-PEPCK and *Asu*-PEPCK, possessed several of the conserved residues in the corresponding regions while existing as monomers. We do note that the recombinant PEPCKs examined here were proteins truncated at their N-termini to remove the predicted transport peptides (30–47 aa length), which were close to regions corresponding to the oligomerization domain in *Tcr*-PEPCK. We thus cannot rule out the possibility that the truncations affected the quaternary structure of the proteins. Indeed, the green alga *Chlamydomonas reinhardtii* only harbors a single gene encoding PEPCK, but produces two isoforms, a hexameric *Cre*-PEPCK1 and a monomeric *Cre*-PEPCK2; it has been postulated that these two isoforms are generated through alternative splicing of the gene transcript or regulated proteolysis of the enzyme (Torresi et al., 2023). Alternative splicing of gene transcripts has also been observed in brown algae (Cormier et al., 2017; Franco et al., 2008; Teng et al., 2024; Wu et al., 2013). Therefore, there is a possibility that the PEPCKs from brown algae also form isoforms in vivo through alternative splicing.

PEPCK is present in all three domains of life and plays important roles in metabolism beyond in the C_4 cycle in C_4 and CAM plants (Leegood & Walker, 2003; Walker et al., 1997; Walker et al., 2021; Yang et al., 2009), including in gluconeogenesis. PEPCK is thus regulated by a variety of metabolites (Leegood & Walker, 2003). The carboxylation activity of *Io*-PEPCK was moderately inhibited by intermediates of the TCA cycle (citrate, succinate, and malate), whereas the same intermediates slightly enhanced the decarboxylation activity (Figure 4). Similar responses were also observed in the PEPCKs from pineapple (Martin et al., 2011), *Arabidopsis thaliana* (Rojas et al., 2019), and *Chlamydomonas reinhardtii* (Torresi et al., 2023), suggesting that accumulation of TCA-cycle intermediates promotes decarboxylation and gluconeogenesis. This regulation may be particularly relevant if the PEPCK proteins from brown algae are localized in the mitochondrion, as suggested by their N-terminal sequences (Table S2). In contrast, the responses of PEPCKs from various organisms to amino acids and intermediates of glycolysis (G6P, FBP, 3-PGA,

and pyruvate) vary. For instance, glutamate inhibited *Arabidopsis thaliana* PEPCK (Rojas et al., 2019) but had little effect on *Io*-PEPCK and PEPCKs from pineapple (Martin et al., 2011) and the C_4 plant *Urochloa panicoides* (Burnell, 1986). Phenylalanine enhanced the decarboxylation activity of *C. reinhardtii* PEPCK (Torresi et al., 2023) but not *Io*-PEPCK. The glycolysis-intermediates FBP and 3-PGA both inhibited the decarboxylation activity of PEPCKs from *Ar. thaliana* (Rojas et al., 2019), pineapple (Martin et al., 2011), and *U. panicoides* (Burnell, 1986), but did not affect *C. reinhardtii* PEPCK (*Cre*-PEPCK1 and 2; Torresi et al., 2023). By contrast, *Io*-PEPCK decarboxylation was promoted by 3-PGA, whereas FBP had little effect.

In many plants, including C_3, C_4, and CAM plants, PEPCK activity is also regulated by phosphorylation: PEPCK is phosphorylated in the dark and reversed by light (Leegood & Walker, 2003; Walker et al., 1997; Walker et al., 2021). PEPCKs that are subject to phosphorylation, such as the PEPCKs from *Ananas comosus* (*Aco*-PEPCK), *Megathyrsus maximus* (*Mma*-PEPCK), *Zea mays* (*Zma*-PEPCK), *Arabidopsis thaliana* (*Ath*-PEPCK), and *Cucumis sativus* (*Csa*-PEPCK; Chao et al., 2014; Leegood & Walker, 2003; Rojas et al., 2019; Shen et al., 2017; Walker et al., 1997; Walker et al., 2002; Walker & Leegood, 1995, 1996), possess an N-terminal extension containing a conserved phosphorylation site (Figure S6). However, the PEPCKs from brown algae did not possess N-terminal extensions and lacked the conserved phosphorylation site motif (Figure S6). Our knowledge at present does not suggest a phosphorylation-mediated regulation of PEPCKs in brown algae.

The concentration of ATP seems to be another factor for the regulation of PEPCK. Our analyses showed that the carboxylation activity of *Io*-PEPCK was subject to a mixed-type inhibition by ATP. Inhibition of PEPCK carboxylation activity with increases in ATP concentration has also been reported in enzymes from other organisms, such as the brown alga *Laminaria hyperborea* (Weidner & Kuppers, 1982), the C_4 plant *Megathyrsus maximus* (Walker et al., 1997; Walker et al., 2002), and the parasite *Trypanosoma cruzi* (Urbina, 1987). The ATP/ADP ratio has also been observed to modulate the affinity of PEPCK for the substrates: Higher ATP/ADP ratios increased the affinity for OAA while decreasing the affinity for PEP (Leegood & Walker, 2003; Walker et al., 2002; Walker & Chen, 2002). These findings suggest that the ATP concentration and/or ATP/ADP ratio may act as signals to regulate PEPCK in vivo and may be important in organisms, including brown algae, that do not utilize phosphorylation as a means to regulate PEPCK activity.

PEPC is responsible for the CO_2 fixation and production of OAA from PEP in the C_4 cycle in C_4 plants (Figure S1). However, many studies have shown that PEPC activity could not be detected in the cell extracts of brown algae, while relatively high levels of PEPCK carboxylation activity were observed (Akagawa, Ikawa, & Nisizawa, 1972a; Busch & Schmid, 2001; Cabello-Pasini et al., 2000; Kremer & Kuppers, 1977). Our analysis of the cell extracts from *Ishige okamurae* also indicated that PEPC activity was very low, only 9% of the observed PEPCK carboxylation activity (Figure 6). The carboxylation activities of purified PEPCKs from brown algae were similar to those of purified PEPCs from C_4 plants, such as maize. The carboxylation activity deriving from PEPCK observed in cell extracts of *I. okamurae* was also comparable to the activity deriving from PEPC in maize extracts (Uedan & Sugiyama, 1976; Willeford et al., 1990). This raises the possibility that PEPCK could play a role in fixing CO_2, similar to the role of PEPC in the C_4 pathway, which has been proposed in the past (Akagawa, Ikawa, & Nisizawa, 1972a). In this case, the simplest scenario would be that PEPCK functions as a carboxylase in the cytosol of *I. okamurae* and possibly other species, replacing the cytosolic PEPC (Figure 7). The generated OAA could be converted to either malate by malate dehydrogenase or to aspartate by aminotransferase in the cytosol, followed by transport to the cells where the CBB cycle and RuBisCO are active. Release of CO_2 can be carried out by either PEPCK or malic enzyme, both capable of mitochondrial localization based on their primary structures with putative signal sequences (Figure 7). In this scenario, however, it would be necessary that PEPCK be present in the cytosol in addition to the mitochondrion. As only a single PEPCK gene has been observed in brown algae (Chi et al., 2014), alternative splicing of the PEPCK gene may occur in *I. okamurae*, resulting in the production of two isoforms of PEPCK (cytosolic and mitochondrial) responsible for the fixation and release of CO_2 in the C_4 cycle-like pathway. Further experimental evidence on alternative splicing and subcellular localization(s) of PEPCKs, along with the activities, and in particular, the localization of other potentially important enzymes such as PEPC and malic enzyme, will be necessary to better understand the mechanisms of CCMs in brown algae.

AUTHOR CONTRIBUTIONS

Jian-qiang Jin: Data curation (lead); formal analysis (equal); investigation (equal); writing – original draft (equal); writing – review and editing (equal). **Yuusuke Yokooji:** Formal analysis (equal); investigation (equal); validation (equal); writing – original draft (equal); writing – review and editing (equal). **Toshiyuki Shibata:** Investigation (supporting); methodology (supporting); writing – review and editing (supporting). **Haruyuki Atomi:** Conceptualization (equal); formal analysis (equal); funding acquisition (equal); project administration (equal); supervision (equal); writing – review and editing (equal).

ACKNOWLEDGMENTS

This work was supported by grants from the New Energy and Industrial Technology Development Organization (NEDO) and Moonshot Research and Development Program (grant number JPNP18016).

DATA AVAILABILITY STATEMENT

NCBI accession numbers for *Es*-, *Io*-, *Sh*-, *Sj*-, and *Sl*-PEPCK are CBJ26625.1, AIT70078.1, AIT70089.1, AIW62929.1, and AIT70085.1, respectively. All relevant data are included in the manuscript and Supporting Information.

ORCID

Haruyuki Atomi https://orcid.org/0000-0001-9687-6426

REFERENCES

Akagawa, H., Ikawa, T., & Nisizawa, K. (1972a). The enzyme system for the entrance of $^{14}CO_2$ in the dark CO_2-fixation of brown algae. *Plant and Cell Physiology*, *13*(6), 999–1016. https://doi.org/10.1093/oxfordjournals.pcp.a074829

Akagawa, H., Ikawa, T., & Nisizawa, K. (1972b). Initial pathway of dark $^{14}CO_2$-fixation in brown algae. *Botanica Marina*, *15*(3), 119–125. https://doi.org/10.1515/botm.1972.15.3.119

Akagawa, H., Nisizawa, K., & Ikawa, T. (1972). $^{14}CO_2$-fixation in marine algae with special reference to dark-fixation in brown algae. *Botanica Marina*, *15*(3), 126–132. https://doi.org/10.1515/botm.1972.15.3.126

Almagro, J. J. A., Salvatore, M., Emanuelsson, O., Winther, O., von Heijne, G., Elofsson, A., & Nielsen, H. (2019). Detecting sequence signals in targeting peptides using deep learning. *Life Science Alliance*, *2*(5), e201900429. https://doi.org/10.26508/lsa.201900429

Andrade, C., Sepulveda, C., Cardemil, E., & Jabalquinto, A. M. (2010). The role of tyrosine 207 in the reaction catalyzed by *Saccharomyces cerevisiae* phosphoenolpyruvate carboxykinase. *Biological Research*, *43*(2), 191–195. https://doi.org/10.4067/S0716-97602010000200007

Burnell, J. (1986). Purification and properties of phospho*enol*pyruvate carboxykinase from C_4 plants. *Functional Plant Biology*, *13*(5), 577–587. https://doi.org/10.1071/PP9860577

Busch, S., & Schmid, R. (2001). Enzymes associated with β-carboxylation in *Ectocarpus siliculosus* (Phaeophyceae): Are they involved in net carbon acquisition. *European Journal of Phycology*, *36*(1), 61–70. https://doi.org/10.1017/S0967026201003067

Cabello-Pasini, A., & Alberte, R. S. (1997). Seasonal patterns of photosynthesis and light-independent carbon fixation in marine macrophytes. *Journal of Phycology*, *33*(3), 321–329. https://doi.org/10.1111/j.0022-3646.1997.00321.x

Cabello-Pasini, A., & Alberte, R. S. (2001a). Enzymatic regulation of photosynthetic and light-independent carbon fixation in *Laminaria setchellii* (Phaeophyta), *Ulva lactuca* (Chlorophyta) and *Iridaea cordata* (Rhodophyta). *Revista Chilena de Historia Natural*, *74*(2), 229–236. https://doi.org/10.4067/S0716-078X2001000200002

Cabello-Pasini, A., & Alberte, R. S. (2001b). Expression of carboxylating enzymes in *Laminaria setchellii* (Phaeophyceae). *Phycologia*, *40*(4), 351–358. https://doi.org/10.2216/i0031-8884-40-4-351.1

Cabello-Pasini, A., Smith, G. J., & Alberte, R. S. (2000). Phosphoenolpyruvate carboxykinase from the marine diatom *Skeletonema costatum* and the phaeophyte *Laminaria setchellii*. I. Isolation and biochemical characterization. *Botanica Marina*, *43*(6), 559–568. https://doi.org/10.1515/Bot.2000.056

Capó-Bauçà, S., Galmés, J., Aguiló-Nicolau, P., Ramis-Pozuelo, S., & Iñiguez, C. (2023). Carbon assimilation in upper subtidal macroalgae is determined by an inverse correlation between Rubisco carboxylation efficiency and CO_2 concentrating mechanism effectiveness. *New Phytologist*, *237*(6), 2027–2038. https://doi.org/10.1111/nph.18623

Capó-Bauçà, S., Iñiguez, C., & Galmés, J. (2024). The diversity and coevolution of Rubisco and CO_2 concentrating mechanisms in marine macrophytes. *New Phytologist*, *241*(6), 2353–2365. https://doi.org/10.1111/nph.19528

Chao, Q., Liu, X. Y., Mei, Y. C., Gao, Z. F., Chen, Y. B., Qian, C. R., Hao, Y.-B., & Wang, B. C. (2014). Light-regulated phosphorylation of maize phosphoenolpyruvate carboxykinase plays a vital role in its activity. *Plant Molecular Biology*, *85*(1–2), 95–105. https://doi.org/10.1007/s11103-014-0171-3

Chi, S., Wu, S., Yu, J., Wang, X., Tang, X., & Liu, T. (2014). Phylogeny of C_4-photosynthesis enzymes based on algal transcriptomic and genomic data supports an archaeal/proteobacterial origin and multiple duplication for most C_4-related genes. *PLoS ONE*, *9*(10), e110154. https://doi.org/10.1371/journal.pone.0110154

Cock, J. M., Sterck, L., Rouzé, P., Scornet, D., Allen, A. E., Amoutzias, G., Anthouard, V., Artiguenave, F., Aury, J.-M., Badger, J. H., Beszteri, B., Billiau, K., Bonnet, E., Bothwell, J. H., Bowler, C., Boyen, C., Brownlee, C., Carrano, C. J., Charrier, B., … Wincker, P. (2010). The *Ectocarpus* genome and the independent evolution of multicellularity in brown algae. *Nature*, *465*(7298), 617–621. https://doi.org/10.1038/nature09016

Cooper, T. G., Tchen, T. T., Wood, H. G., & Benedict, C. R. (1968). The carboxylation of phosphoenolpyruvate and pyruvate. I. The active species of "CO_2" utilized by phosphoenolpyruvate carboxykinase, carboxytransphosphorylase, and pyruvate carboxylase. *Journal of Biological Chemistry*, *243*(14), 3857–3863.

Cormier, A., Avia, K., Sterck, L., Derrien, T., Wucher, V., Andres, G., Monsoor, M., Godfroy, O., Lipinska, A., Perrineau, M. M., Van De Peer, Y., Hitte, C., Corre, E., Coelho, S. M., & Cock, J. M. (2017). Re-annotation, improved large-scale assembly and establishment of a catalogue of noncoding loci for the genome of the model brown alga *Ectocarpus*. *New Phytologist*, *214*(1), 219–232. https://doi.org/10.1111/nph.14321

Cotelesage, J. J., Puttick, J., Goldie, H., Rajabi, B., Novakovski, B., & Delbaere, L. T. (2007). How does an enzyme recognize CO_2? *International Journal of Biochemistry & Cell Biology*, *39*(6), 1204–1210. https://doi.org/10.1016/j.biocel.2007.03.015

Craigie, J. (1963). Dark fixation of C^{14}-bicarbonate by marine algae. *Canadian Journal of Botany*, *41*(3), 317–325. https://doi.org/10.1139/b63-029

Cymeryng, C., Cazzulo, J. J., & Cannata, J. J. (1995). Phospho*enol*pyruvate carboxykinase from *Trypanosoma cruzi*. Purification and physicochemical and kinetic properties. *Molecular and Biochemical Parasitology*, *73*(1–2), 91–101. https://doi.org/10.1016/0166-6851(95)00099-m

Daley, L. S., Ray, T. B., Vines, H. M., & Black, C. C. (1977). Characterization of phosphoenolpyruvate carboxykinase from pineapple leaves *Ananas comosus* (L.) Merr. *Plant Physiology*, *59*(4), 618–622. https://doi.org/10.1104/pp.59.4.618

Delbaere, L. T., Sudom, A. M., Prasad, L., Leduc, Y., & Goldie, H. (2004). Structure/function studies of phosphoryl transfer by phosphoenolpyruvate carboxykinase. *Biochimica et Biophysica Acta*, *1697*(1–2), 271–278. https://doi.org/10.1016/j.bbapap.2003.11.030

Duarte, C. M., Gattuso, J. P., Hancke, K., Gundersen, H., Filbee-Dexter, K., Pedersen, M. F., & Krause-Jensen, D. (2022). Global estimates of the extent and production of macroalgal forests. *Global Ecology and Biogeography*, *31*(7), 1422–1439. https://doi.org/10.1111/geb.13515

Duarte, C. M., Losada, I. J., Hendriks, I. E., Mazarrasa, I., & Marbà, N. (2013). The role of coastal plant communities for climate change mitigation and adaptation. *Nature Climate Change*, *3*(11), 961–968. https://doi.org/10.1038/Nclimate1970

Dunten, P., Belunis, C., Crowther, R., Hollfelder, K., Kammlott, U., Levin, W., Michel, H., Ramsey, G. B., Swain, A., Weber, D., & Wertheimer, S. J. (2002). Crystal structure of human cytosolic phosphoenolpyruvate carboxykinase reveals a new GTP-binding site. *Journal of Molecular Biology*, *316*(2), 257–264. https://doi.org/10.1006/jmbi.2001.5364

Franco, P. O., Rousvoal, S., Tonon, T., & Boyen, C. (2008). Whole genome survey of the glutathione transferase family in the brown algal model *Ectocarpus siliculosus*. *Marine Genomics*, *1*(3–4), 135–148. https://doi.org/10.1016/j.margen.2009.01.003

Fukuda, W., Fukui, T., Atomi, H., & Imanaka, T. (2004). First characterization of an archaeal GTP-dependent phosphoenolpyruvate carboxykinase from the hyperthermophilic archaeon *Thermococcus kodakaraensis* KOD1. *Journal of Bacteriology*, *186*(14), 4620–4627. https://doi.org/10.1128/Jb.186.14.4620-4627.2004

Furbank, R. T. (2011). Evolution of the C_4 photosynthetic mechanism: Are there really three C_4 acid decarboxylation types? *Journal of Experimental Botany*, *62*(9), 3103–3108. https://doi.org/10.1093/jxb/err080

Furbank, R. T. (2016). Walking the C_4 pathway: Past, present, and future. *Journal of Experimental Botany*, *67*(14), 4057–4066. https://doi.org/10.1093/jxb/erw161

Gómez, I., & Huovinen, P. (2012). Morpho-functionality of carbon metabolism in seaweeds. In C. Wiencke & K. Bischof (Eds.), *Seaweed biology: Novel insights into ecophysiology, ecology and utilization* (pp. 25–46). Springer. https://doi.org/10.1007/978-3-642-28451-9_2

Gómez, I., Orostegui, M., & Huovinen, P. (2007). Morpho-functional patterns of photosynthesis in the south pacific kelp *Lessonia nigrescens*: Effects of UV radiation on ^{14}C fixation and primary photochemical reactions. *Journal of Phycology*, *43*(1), 55–64. https://doi.org/10.1111/j.1529-8817.2006.00301.x

Gravot, A., Dittami, S. M., Rousvoal, S., Lugan, R., Eggert, A., Collén, J., Boyen, C., Bouchereau, A., & Tonon, T. (2010). Diurnal oscillations of metabolite abundances and gene analysis provide new insights into central metabolic processes of the brown alga *Ectocarpus siliculosus*. *New Phytologist*, *188*(1), 98–110. https://doi.org/10.1111/j.1469-8137.2010.03400.x

Griscom, B. W., Adams, J., Ellis, P. W., Houghton, R. A., Lomax, G., Miteva, D. A., Schlesinger, W. H., Shoch, D., Siikamäki, J. V., Smith, P., Woodbury, P., Zganjar, C., Blackman, A., Campari, J., Conant, R. T., Delgado, C., Elias, P., Gopalakrishna, T., Hamsik, M. R., … Fargione, J. (2017). Natural climate solutions. *Proceedings of the National Academy of Sciences of the United States of America*, *114*(44), 11645–11650. https://doi.org/10.1073/pnas.1710465114

Holbrook, G. P., Beer, S., Spencer, W. E., Reiskind, J. B., Davis, J. S., & Bowes, G. (1988). Photosynthesis in marine macroalgae: Evidence for carbon limitation. *Canadian Journal of Botany*, *66*(3), 577–582. https://doi.org/10.1139/b88-083

Iñiguez, C., Capó-Bauçà, S., Niinemets, Ü., Stoll, H., Aguiló-Nicolau, P., & Galmés, J. (2020). Evolutionary trends in RuBisCO kinetics and their co-evolution with CO_2 concentrating mechanisms. *Plant Journal*, *101*(4), 897–918. https://doi.org/10.1111/tpj.14643

Johnston, A. M., & Raven, J. A. (1989). Extraction, partial purification and characterization of phosphoenolpyruvate carboxykinase from *Ascophyllum nodosum* (Phaeophyceae). *Journal of Phycology*, *25*(3), 568–576. https://doi.org/10.1111/j.1529-8817.1989.tb00263.x

Jones, D. T., Taylor, W. R., & Thornton, J. M. (1992). The rapid generation of mutation data matrices from protein sequences. *Computer Applications in the Biosciences*, *8*(3), 275–282. https://doi.org/10.1093/bioinformatics/8.3.275

Joshi, G., Gee, R., Saltman, P., & Dolan, T. (1962). Sodium chloride effect on dark fixation of CO_2 by marine & terrestrial plants. *Plant Physiology*, *37*(3), 446–449. https://doi.org/10.1104/pp.37.3.446

Koch, M., Bowes, G., Ross, C., & Zhang, X. H. (2013). Climate change and ocean acidification effects on seagrasses and marine macroalgae. *Global Change Biology*, *19*(1), 103–132. https://doi.org/10.1111/j.1365-2486.2012.02791.x

Krause-Jensen, D., & Duarte, C. M. (2016). Substantial role of macroalgae in marine carbon sequestration. *Nature Geoscience*, *9*(10), 737–742. https://doi.org/10.1038/Ngeo2790

Kremer, B. P. (1981a). C_4-metabolism in marine brown macrophytic algae. *Zeitschrift für Naturforschung. Section C*, *36*(9–10), 840–847. https://doi.org/10.1515/znc-1981-9-1024

Kremer, B. P. (1981b). Metabolic implications of non-photosynthetic carbon fixation in brown macroalgae. *Phycologia*, *20*(3), 242–250. https://doi.org/10.2216/i0031-8884-20-3-242.1

Kremer, B. P., & Kuppers, U. (1977). Carboxylating enzymes and pathway of photosynthetic carbon assmilation in different marine algae—Evidence for the C_4-pathway? *Planta*, *133*(2), 191–196. https://doi.org/10.1007/BF00391918

Larkin, M. A., Blackshields, G., Brown, N. P., Chenna, R., McGettigan, P. A., McWilliam, H., Valentin, F., Wallace, I. M., Wilm, A., Lopez, R., Thompson, J. D., Gibson, T. J., & Higgins, D. G. (2007). Clustal W and Clustal X version 2.0. *Bioinformatics*, *23*(21), 2947–2948. https://doi.org/10.1093/bioinformatics/btm404

Lee, M. H., Hebda, C. A., & Nowak, T. (1981). The role of cations in avian liver phosphoenolpyruvate carboxykinase catalysis. Activation and regulation. *Journal of Biological Chemistry*, *256*(24), 12793–12801. https://doi.org/10.1016/S0021-9258(18)42965-1

Leegood, R. C., & Walker, R. P. (2003). Regulation and roles of phospho*enol*pyruvate carboxykinase in plants. *Archives of Biochemistry and Biophysics*, *414*(2), 204–210. https://doi.org/10.1016/s0003-9861(03)00093-6

Lin, P., Yao, Y., Lu, L., Bi, Y., & Zhou, Z. (2025). The isolation and functional identification of a phosphoenolpyruvate carboxykinase gene from *Saccharina japonica*. *Aquaculture and Fisheries*, *10*(2), 210–218. https://doi.org/10.1016/j.aaf.2023.08.007

Maberly, S. C., & Gontero, B. (2017). Ecological imperatives for aquatic CO_2-concentrating mechanisms. *Journal of Experimental Botany*, *68*(14), 3797–3814. https://doi.org/10.1093/jxb/erx201

Martin, M., Rius, S. P., & Podesta, F. E. (2011). Two phosphoenolpyruvate carboxykinases coexist in the crassulacean acid metabolism plant *Ananas comosus*. Isolation and characterization of the smaller 65 kDa form. *Plant Physiology and Biochemistry*, *49*(6), 646–653. https://doi.org/10.1016/j.plaphy.2011.02.015

Matte, A., Goldie, H., Sweet, R. M., & Delbaere, L. T. (1996). Crystal structure of *Escherichia coli* phosphoenolpyruvate carboxykinase: A new structural family with the P-loop nucleoside triphosphate hydrolase fold. *Journal of Molecular Biology*, *256*(1), 126–143. https://doi.org/10.1006/jmbi.1996.0072

Matte, A., Tari, L. W., Goldie, H., & Delbaere, L. T. (1997). Structure and mechanism of phosphoenolpyruvate carboxykinase. *Journal of Biological Chemistry*, *272*(13), 8105–8108. https://doi.org/10.1074/jbc.272.13.8105

McLeod, M. J., & Holyoak, T. (2021). Enzymes | phosphoenolpyruvate Carboxykinases. In J. Jez (Ed.), *Encyclopedia of biological chemistry III* (3rd ed., pp. 400–412). Elsevier. https://doi.org/10.1016/B978-0-12-819460-7.00226-7

McLeod, M. J., & Holyoak, T. (2023). Biochemical, structural, and kinetic characterization of PP_i-dependent phosphoenolpyruvate carboxykinase from *Propionibacterium freudenreichii*. *Proteins*, *91*(9), 1261–1275. https://doi.org/10.1002/prot.26513

Meyer, M., & Griffiths, H. (2013). Origins and diversity of eukaryotic CO_2-concentrating mechanisms: Lessons for the future.

Journal of Experimental Botany, *64*(3), 769–786. https://doi.org/10.1093/jxb/ers390

Miller, R. S., & Lane, M. D. (1968). The enzymatic carboxylation of phosphoenolpyruvate. V. Kinetic and ^{18}O studies on liver mitochondrial phosphoenolpyruvate carboxykinase. *Journal of Biological Chemistry*, *243*(22), 6041–6049.

Nellemann, C., Corcoran, E., Duarte, C. M., Valdés, L., De Young, C., Fonseca, L., & Grimsditch, G. (2009). *Blue carbon: The role of healthy oceans in binding carbon: a rapid response assessment*. United Nations Environmental Programme and GRID-Arendal. https://www.grida.no/publications/145

Oh, Z. G., Askey, B., & Gunn, L. H. (2023). Red Rubiscos and opportunities for engineering green plants. *Journal of Experimental Botany*, *74*(2), 520–542. https://doi.org/10.1093/jxb/erac349

Pessarrodona, A., Franco-Santos, R. M., Wright, L. S., Vanderklift, M. A., Howard, J., Pidgeon, E., Wernberg, T., & Filbee-Dexter, K. (2023). Carbon sequestration and climate change mitigation using macroalgae: A state of knowledge review. *Biological Reviews*, *98*(6), 1945–1971. https://doi.org/10.1111/brv.12990

Podkovyrov, S. M., & Zeikus, J. G. (1993). Purification and characterization of phosphoenolpyruvate carboxykinase,a catabolic CO_2-fixing enzyme, from *Anaerobiospirillum succiniciproducens*. *Journal of General Microbiology*, *139*(2), 223–228. https://doi.org/10.1099/00221287-139-2-223

Rao, X. L., & Dixon, R. A. (2016). The differences between NAD-ME and NADP-ME subtypes of C_4 photosynthesis: More than decarboxylating enzymes. *Frontiers in Plant Science*, *7*, 1525. https://doi.org/10.3389/fpls.2016.01525

Raven, J. A., & Giordano, M. (2017). Acquisition and metabolism of carbon in the Ochrophyta other than diatoms. *Philosophical Transactions of the Royal Society B*, *372*(1728), 20160400. https://doi.org/10.1098/rstb.2016.0400

Robert, X., & Gouet, P. (2014). Deciphering key features in protein structures with the new ENDscript server. *Nucleic Acids Research*, *42*(Web Server issue), W320–W324. https://doi.org/10.1093/nar/gku316

Rojas, B. E., Hartman, M. D., Figueroa, C. M., Leaden, L., Podesta, F. E., & Iglesias, A. A. (2019). Biochemical characterization of phospho*enol*pyruvate carboxykinases from *Arabidopsis thaliana*. *Biochemical Journal*, *476*(20), 2939–2952. https://doi.org/10.1042/BCJ20190523

Shao, Z., Wang, W., Zhang, P., Yao, J., Wang, F., & Duan, D. (2019). Genome-wide identification of genes involved in carbon fixation in *Saccharina japonica* and responses of putative C_4-related genes to bicarbonate concentration and light intensity. *Plant Physiology and Biochemistry*, *137*, 75–83. https://doi.org/10.1016/j.plaphy.2019.01.032

Shen, Z., Dong, X. M., Gao, Z. F., Chao, Q., & Wang, B. C. (2017). Phylogenic and phosphorylation regulation difference of phosphoenolpyruvate carboxykinase of C_3 and C_4 plants. *Journal of Plant Physiology*, *213*, 16–22. https://doi.org/10.1016/j.jplph.2017.02.008

Stepien, C. C., Pfister, C. A., & Wootton, J. T. (2016). Functional traits for carbon access in macrophytes. *PLoS ONE*, *11*(7), e0159062. https://doi.org/10.1371/journal.pone.0159062

Sudom, A., Walters, R., Pastushok, L., Goldie, D., Prasad, L., Delbaere, L. T., & Goldie, H. (2003). Mechanisms of activation of phosphoenolpyruvate carboxykinase from *Escherichia coli* by Ca^{2+} and of desensitization by trypsin. *Journal of Bacteriology*, *185*(14), 4233–4242. https://doi.org/10.1128/JB.185.14.4233-4242.2003

Sudom, A. M., Prasad, L., Goldie, H., & Delbaere, L. T. (2001). The phosphoryl-transfer mechanism of *Escherichia coli* phosphoenolpyruvate carboxykinase from the use of AlF_3. *Journal of Molecular Biology*, *314*(1), 83–92. https://doi.org/10.1006/jmbi.2001.5120

Tamura, K., Stecher, G., & Kumar, S. (2021). MEGA11: Molecular evolutionary genetics analysis version 11. *Molecular Biology and Evolution*, *38*(7), 3022–3027. https://doi.org/10.1093/molbev/msab120

Tari, L. W., Matte, A., Goldie, H., & Delbaere, L. T. (1997). Mg^{2+}–Mn^{2+} clusters in enzyme-catalyzed phosphoryl-transfer reactions. *Nature Structural Biology*, *4*(12), 990–994. https://doi.org/10.1038/nsb1297-990

Tari, L. W., Matte, A., Pugazhenthi, U., Goldie, H., & Delbaere, L. T. (1996). Snapshot of an enzyme reaction intermediate in the structure of the ATP-Mg^{2+}-oxalate ternary complex of *Escherichia coli* PEP carboxykinase. *Nature Structural Biology*, *3*(4), 355–363. https://doi.org/10.1038/nsb0496-355

Teng, L., Sun, Y., Chen, J., Wang, C., Urbach, J. M., Kobe, B., Ye, N., & Zeng, Q. (2024). Exon shuffling and alternative splicing of ROCO genes in brown algae enables a diverse repertoire of candidate immune receptors. *Frontiers in Plant Science*, *15*, 1445022. https://doi.org/10.3389/fpls.2024.1445022

Thumuluri, V., Almagro Armenteros, J. J., Johansen, A. R., Nielsen, H., & Winther, O. (2022). DeepLoc 2.0: Multi-label subcellular localization prediction using protein language models. *Nucleic Acids Research*, *50*(W1), W228–W234. https://doi.org/10.1093/nar/gkac278

Torresi, F., Rodriguez, F. M., Gomez-Casati, D. F., & Martin, M. (2023). Two phosphoenolpyruvate carboxykinases with differing biochemical properties in *Chlamydomonas reinhardtii*. *FEBS Letters*, *597*(4), 585–597. https://doi.org/10.1002/1873-3468.14590

Trapani, S., Linss, J., Goldenberg, S., Fischer, H., Craievich, A. F., & Oliva, G. (2001). Crystal structure of the dimeric phosphoenolpyruvate carboxykinase (PEPCK) from *Trypanosoma cruzi* at 2 Å resolution. *Journal of Molecular Biology*, *313*(5), 1059–1072. https://doi.org/10.1006/jmbi.2001.5093

Uedan, K., & Sugiyama, T. (1976). Purification and characterization of phosphoenolpyruvate carboxylase from maize leaves. *Plant Physiology*, *57*(6), 906–910. https://doi.org/10.1104/pp.57.6.906

Urbina, J. A. (1987). The phospho*enol*pyruvate carboxykinase of *Trypanosoma* (*Schizotrypanum*) *cruzi* epimastigotes: Molecular, kinetic, and regulatory properties. *Archives of Biochemistry and Biophysics*, *258*(1), 186–195. https://doi.org/10.1016/0003-9861(87)90335-3

Wahbeh, M. I., Mahasneh, D. M., & Mahasneh, I. (1985). Concentrations of zinc, manganese, copper, cadmium, magnesium and iron in ten species of algae and sea water from Aqaba, Jordan. *Marine Environmental Research*, *16*(2), 95–102.

Walker, R. P., Acheson, R. M., Tecsi, L. I., & Leegood, R. C. (1997). Phospho*enol*pyruvate carboxykinase in C_4 plants: Its role and regulation. *Australian Journal of Plant Physiology*, *24*(4), 459–468. https://doi.org/10.1071/Pp97007

Walker, R. P., & Chen, Z. H. (2002). Phosphoenolpyruvate carboxykinase: Structure, function and regulation. *Advances in Botanical Research*, *38*, 93–189. https://doi.org/10.1016/S0065-2296(02)38029-7

Walker, R. P., Chen, Z. H., Acheson, R. M., & Leegood, R. C. (2002). Effects of phosphorylation on phospho*enol*pyruvate carboxykinase from the C_4 plant Guinea grass. *Plant Physiology*, *128*(1), 165–172. https://doi.org/10.1104/pp.010432

Walker, R. P., Chen, Z. H., & Famiani, F. (2021). Gluconeogenesis in plants: A key interface between organic acid/amino acid/lipid and sugar metabolism. *Molecules*, *26*(17), 5129. https://doi.org/10.3390/molecules26175129

Walker, R. P., & Leegood, R. C. (1995). Purification, and phosphorylation in vivo and in vitro, of phospho*enol*pyruvate carboxykinase from cucumber cotyledons. *FEBS Letters*, *362*(1), 70–74. https://doi.org/10.1016/0014-5793(95)00212-r

Walker, R. P., & Leegood, R. C. (1996). Phosphorylation of phosphoenolpyruvate carboxykinase in plants. Studies in plants with C_4 photosynthesis and crassulacean acid metabolism and in germinating seeds. *Biochemical Journal*, *317*(Pt 3), 653–658. https://doi.org/10.1042/bj3170653

Walker, R. P., Trevanion, S. J., & Leegood, R. C. (1995). Phosphoenolpyruvate carboxykinase from higher plants: Purification from cucumber and evidence of rapid proteolytic cleavage in extracts from a range of plant-tissues. *Planta*, *196*(1), 58–63. https://doi.org/10.1007/BF00193217

Wang, Y., Brautigam, A., Weber, A. P., & Zhu, X. G. (2014). Three distinct biochemical subtypes of C_4 photosynthesis? A modelling analysis. *Journal of Experimental Botany*, *65*(13), 3567–3578. https://doi.org/10.1093/jxb/eru058

Weidner, M., & Kuppers, U. (1982). Metabolic conversion of ^{14}C-aspartate, ^{14}C-labeled malate and ^{14}C-labeled mannitol by tissue disks of *Laminaria hyperborea*: Role of phosphoenolpyruvate carboxykinase. *Zeitschrift für Pflanzenphysiologie*, *108*(4), 353–364. https://doi.org/10.1016/S0044-328x(82)80181-5

Willeford, K. O., Wu, M. X., Meyer, C. R., & Wedding, R. T. (1990). The role of oligomerization in regulation of maize phosphoenolpyruvate carboxylase activity. Influence of Mg-PEP and malate on the oligomeric equilibrium of PEP carboxylase. *Biochemical and Biophysical Research Communications*, *168*(2), 778–785. https://doi.org/10.1016/0006-291x(90)92389-h

Willenbrink, J., Rangoni-Kubbeler, M., & Tersky, B. (1975). Frond development and CO_2-fixation in *Laminaria hyperborea*. *Planta*, *125*(2), 161–170. https://doi.org/10.1007/BF00388702

Wu, X., Tronholm, A., Caceres, E. F., Tovar-Corona, J. M., Chen, L., Urrutia, A. O., & Hurst, L. D. (2013). Evidence for deep phylogenetic conservation of exonic splice-related constraints: Splice-related skews at exonic ends in the brown alga *Ectocarpus* are common and resemble those seen in humans. *Genome Biology and Evolution*, *5*(9), 1731–1745. https://doi.org/10.1093/gbe/evt115

Yang, J. Q., Kalhan, S. C., & Hanson, R. W. (2009). What is the metabolic role of phosphoenolpyruvate carboxykinase? *Journal of Biological Chemistry*, *284*(40), 27025–27029. https://doi.org/10.1074/jbc.R109.040543

SUPPORTING INFORMATION

Additional supporting information can be found online in the Supporting Information section at the end of this article.

Figure S1. C_4 cycles in C_4 plants.
Figure S2. Amino acid sequences of the PEPCKs selected from five brown algae and their synthesized gene sequences.
Figure S3. Construction of expression plasmids of PEPCKs.
Figure S4. Oligomerization analysis of recombinant PEPCK proteins.
Figure S5. Primary structure analysis of PEPCKs from various brown algae.
Figure S6. Amino acid sequence alignment of ATP-dependent PEPCKs from various organisms.
Figure S7. SDS-PAGE analysis of the purified PEPCK proteins.
Figure S8. Carboxylation activities of PEPCK proteins toward ADP and GDP.
Figure S9. Effect of various metal ions on the carboxylation activity of PEPCK proteins.
Figure S10. Effect of pH on the carboxylation (a) and decarboxylation (b) of PEPCK proteins.
Figure S11. Kinetic analysis of the carboxylating reactions catalyzed by purified PEPCK proteins.
Figure S12. Proposed model of ATP inhibition.
Table S1. Primers used in this study.
Table S2. Predicted localizations of the five brown algal PEPCKs.
Table S3. Activity of ATP-dependent PEPCKs from various organisms.

How to cite this article: Jin, J.-q., Yokooji, Y., Shibata, T., & Atomi, H. (2025). Biochemical characterization of phosphoenolpyruvate carboxykinases from multiple species of brown algae. *Journal of Phycology*, *61*, 1321–1338. https://doi.org/10.1111/jpy.70069